SKAによる宇宙論
multi-tracer method

高橋慶太郎
熊本大学
２０１４年３月２５日

目次

１、宇宙論の現状

標準宇宙モデル

Planck HP

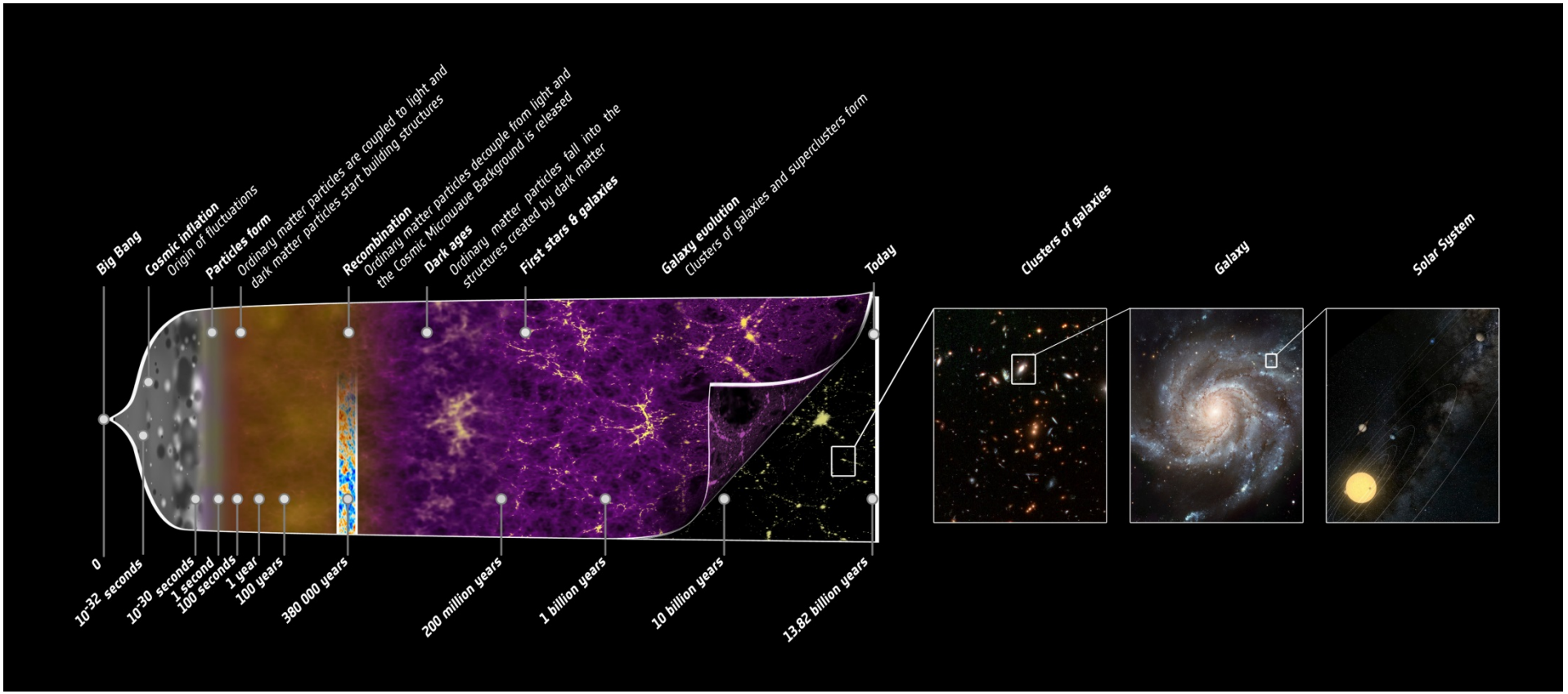

- インフレーションで密度ゆらぎ生成
- 平坦
- 冷たい暗黒物質
- 宇宙定数

宇宙論パラメータ

密度ゆらぎの初期条件

$A \sim 10^{-9}$：大きさ

$n_s \sim 0.96$：スペクトル

宇宙の構成と膨張

$\Omega_c \sim 0.27$：暗黒物質

$\Omega_b \sim 0.05$：バリオン

$\Omega_\Lambda = 1 - \Omega_c - \Omega_b \sim 0.7$：宇宙定数

$H_0 \sim 70\mathrm{km/s/Mpc}$：現在の宇宙膨張速度

再イオン化

$z_{re} \sim 10$：再イオン化の時期

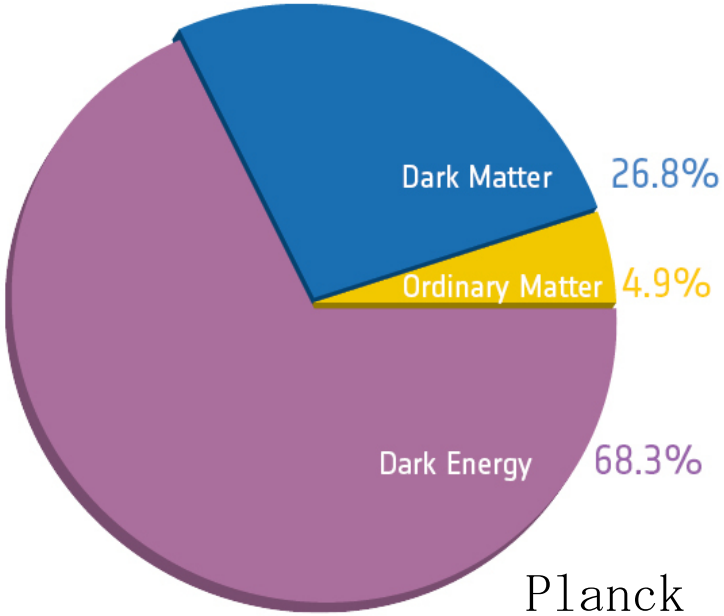

Planck

宇宙論パラメータ

密度ゆらぎの初期条件

$A \sim 10^{-9}$：大きさ

$n_s \sim 0.96$：スペクトル

宇宙の構成と膨張

$\Omega_c \sim 0.27$：暗黒物質

$\Omega_b \sim 0.05$：バリオン

$\Omega_\Lambda = 1 - \Omega_c - \Omega_b \sim 0.7$：

$H_0 \sim 70$km/s/Mpc：現在の宇

再イオン化

$z_{re} \sim 10$：再イオン化の時期

重力波

$r = 0.2$???

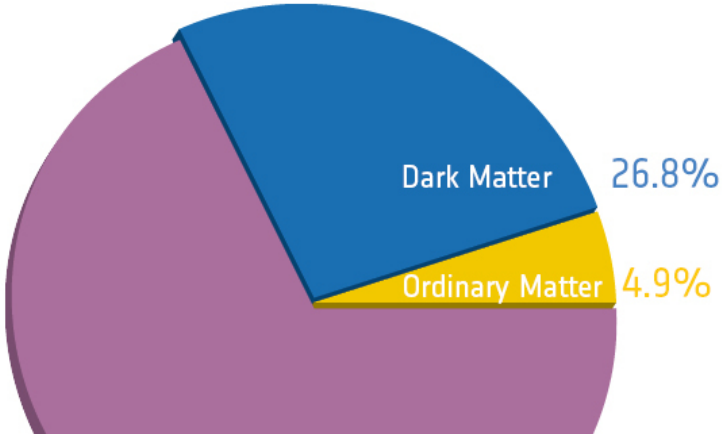

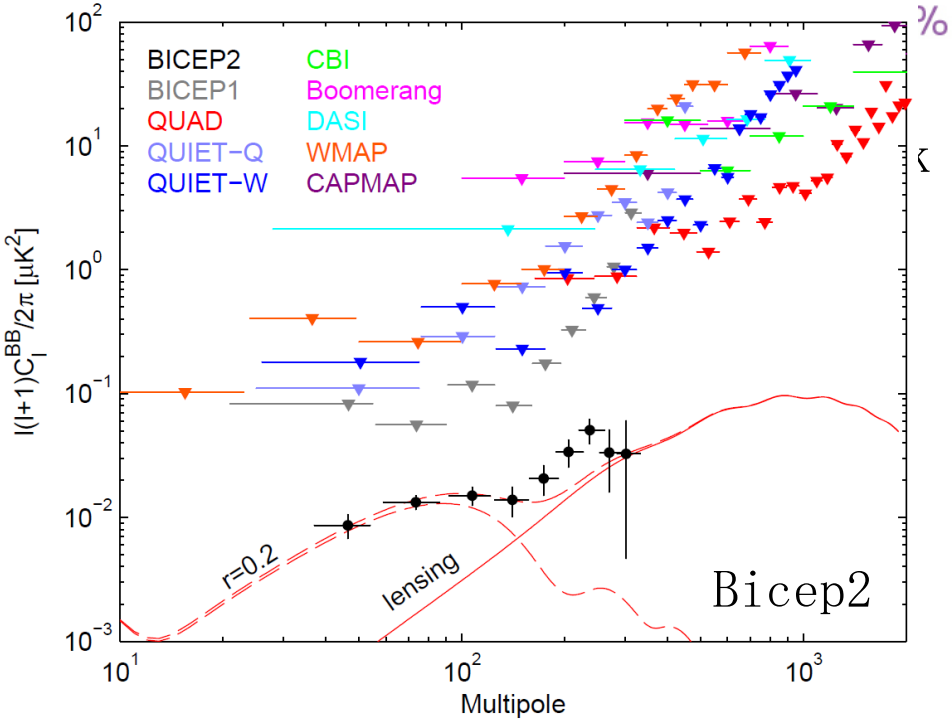

宇宙論の観測

宇宙背景放射
Ia型超新星
銀河分布
弱い重力レンズ

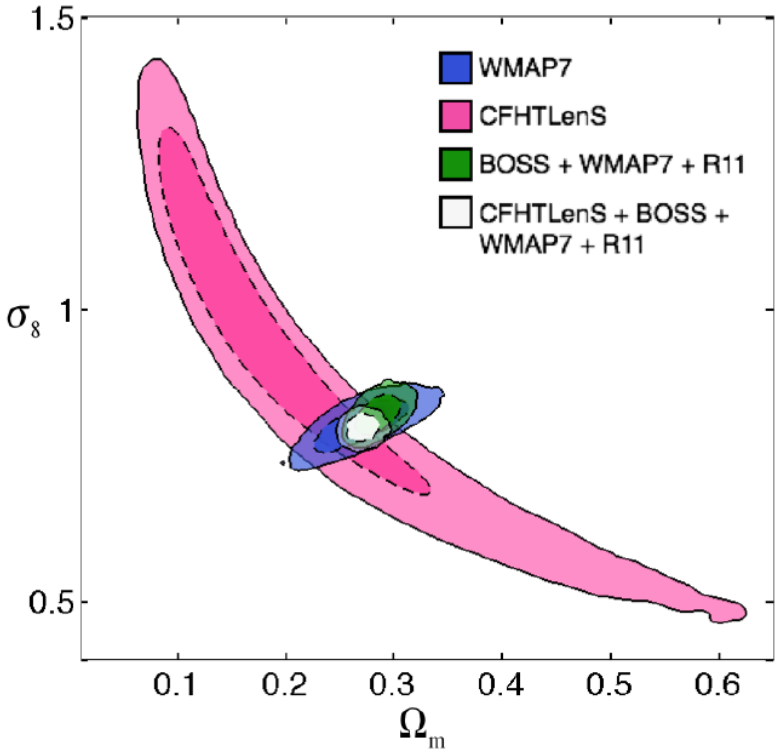

Heymans+ 2013

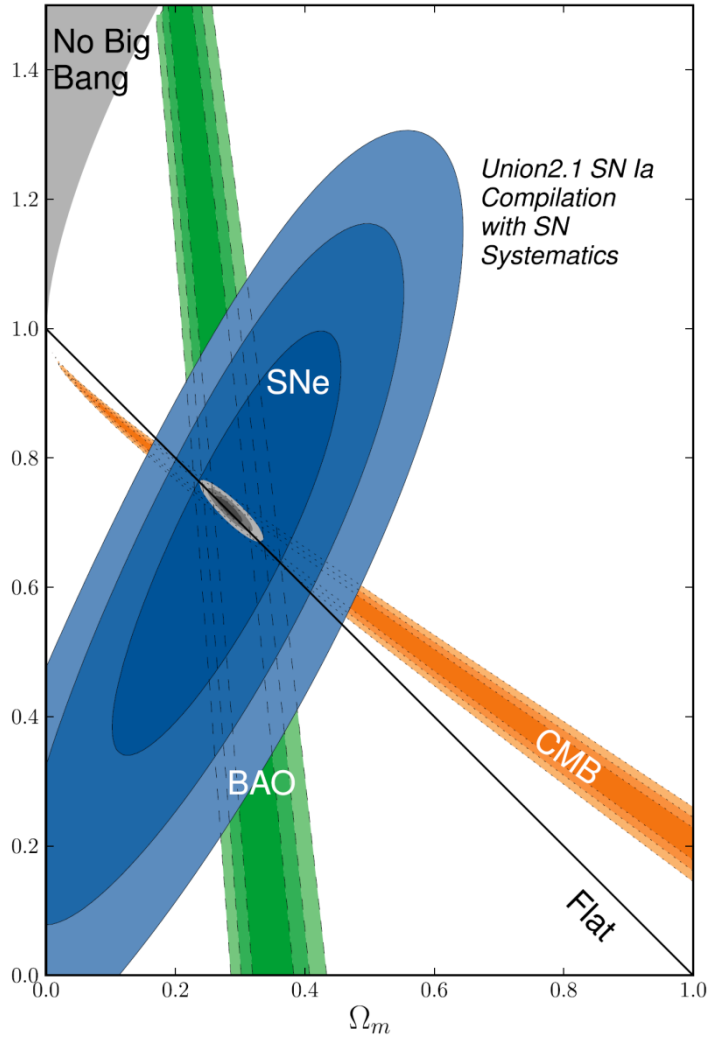

supernova cosmology project 2011

宇宙論：５つの重要問題

暗黒エネルギー（修正重力理論）

暗黒物質
ニュートリノ質量
} 素粒子物理

原始密度ゆらぎの性質
背景重力波
} インフレーション

原始密度ゆらぎの性質

インフレーションによるゆらぎの生成
- ほぼスケール不変
  → ずれが測られている
- ほぼガウス分布
  → まだずれ（非ガウス性）は見えていない

Planck

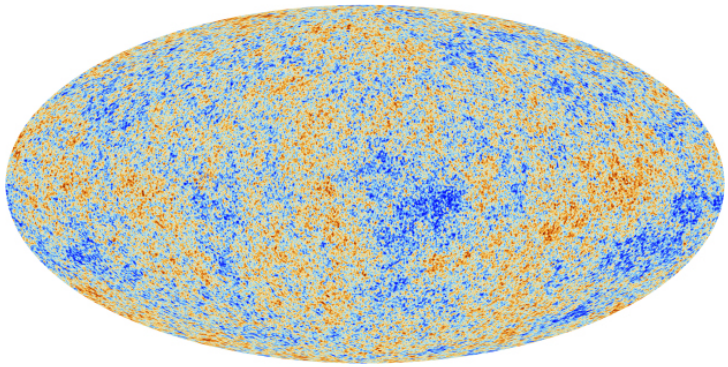

赤が多い？
青が多い？

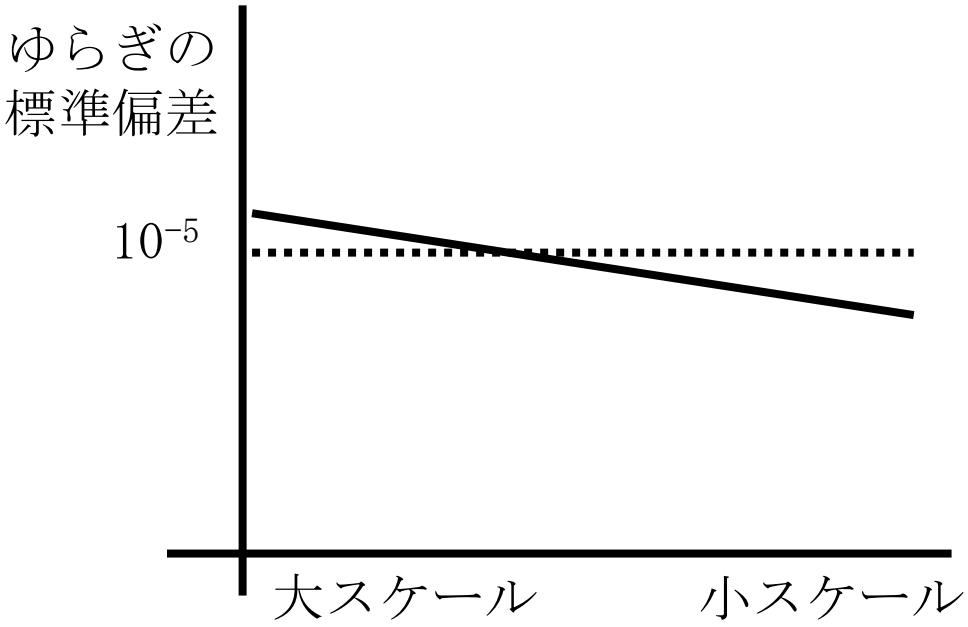

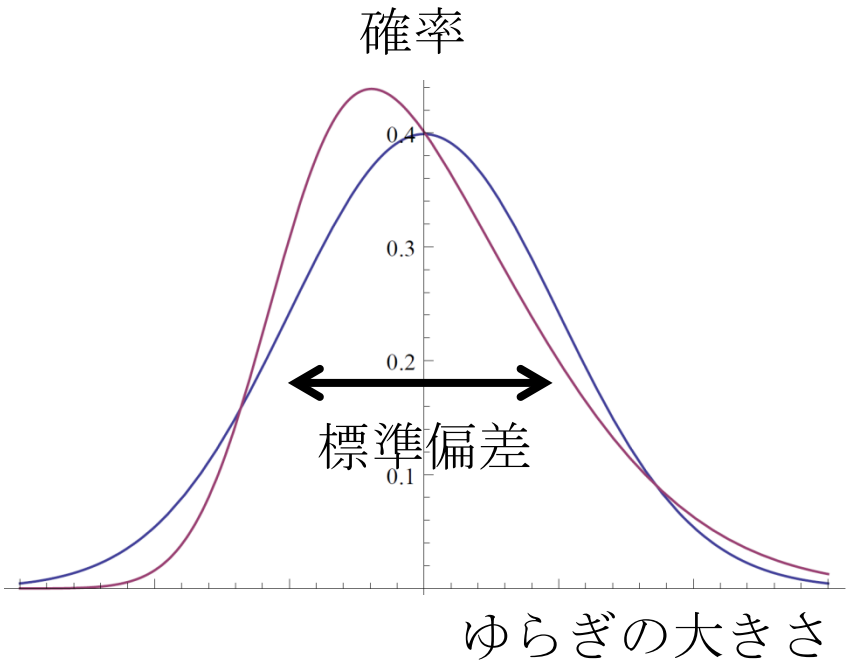

原始密度ゆらぎの性質

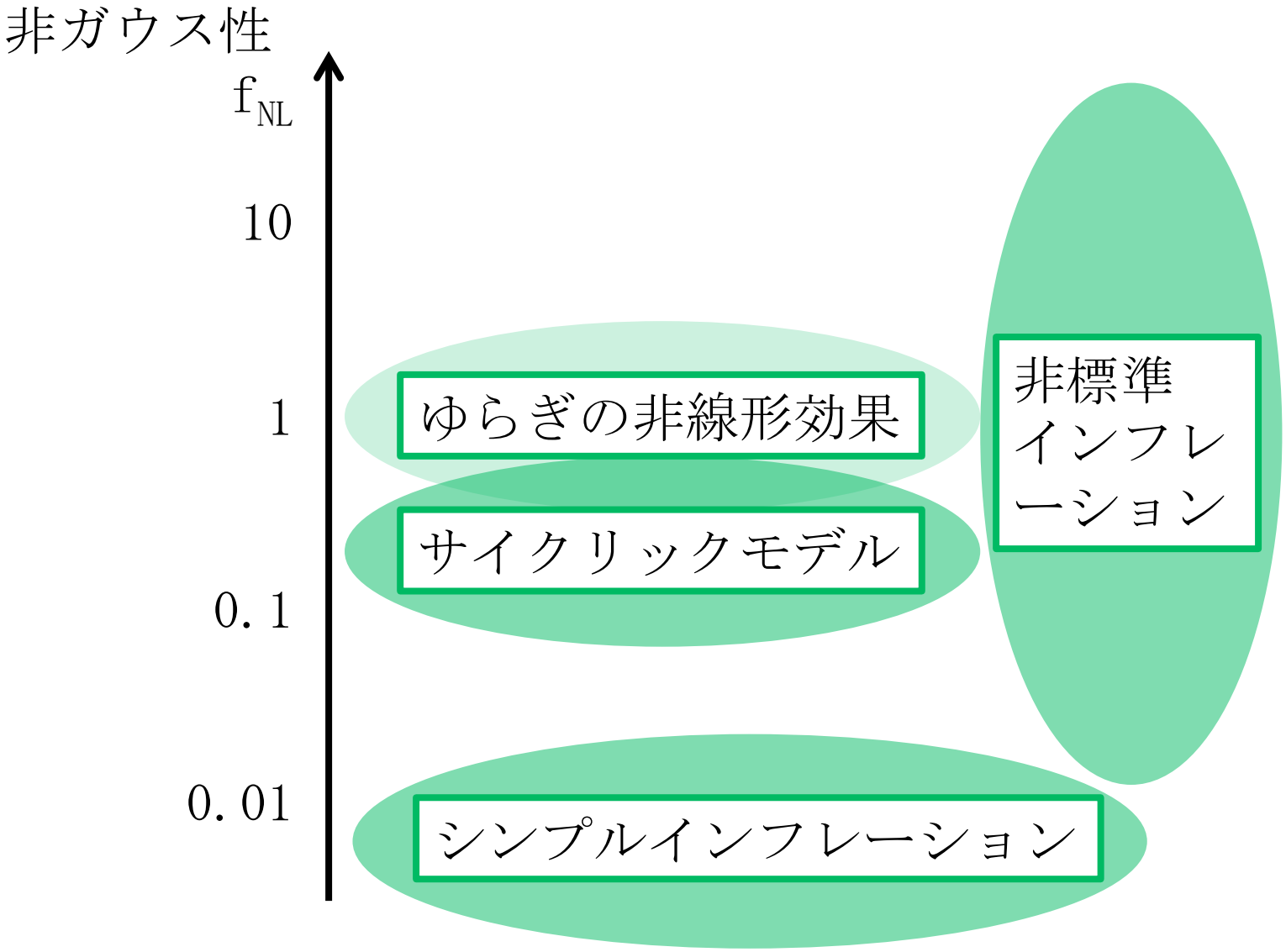
非ガウス性
f_{NL}
10
1
0.1
0.01
ゆらぎの非線形効果
サイクリックモデル
シンプルインフレーション
非標準
インフレ
ーション

原始密度ゆらぎの性質

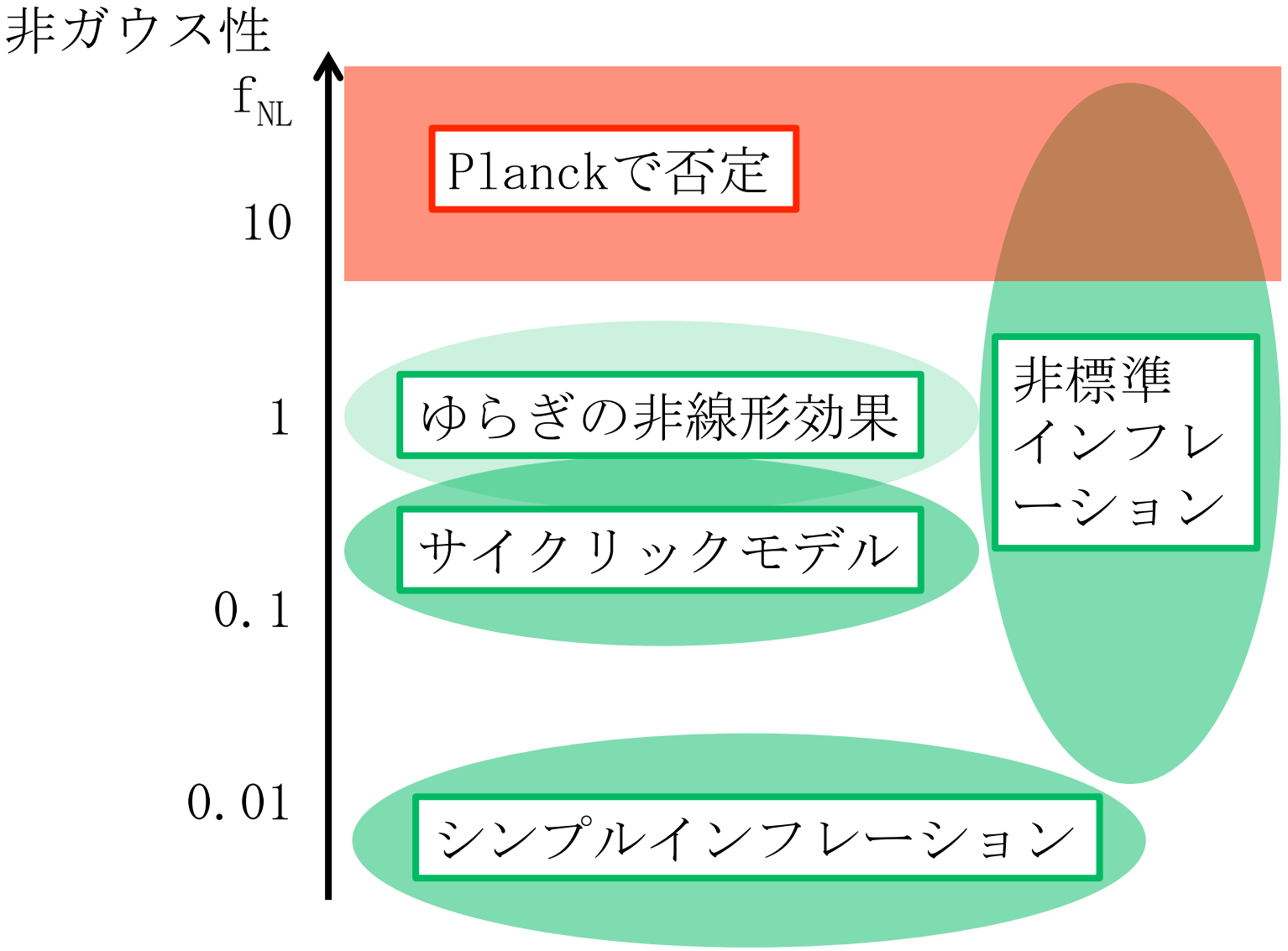
非ガウス性
f_{NL}
10
1
0.1
0.01
Planckで否定
ゆらぎの非線形効果
サイクリックモデル
非標準
インフレ
ーション
シンプルインフレーション

インフレーションの検証

☑スケール不変な密度ゆらぎ
☑スケール不変からの微妙なずれ
☑背景重力波
☐背景重力波のスペクトル → LiteBIRD?
☐密度ゆらぎの非ガウス性 → SKA+光赤外?

2020年代のサーベイ計画

名称	機関	稼働	形態	目的
Euclid	ESA	2020-	人工衛星	暗黒エネルギー
LSST	USA	2022-	地上望遠鏡	汎用
WFIRST	NASA	2023-	人工衛星	汎用

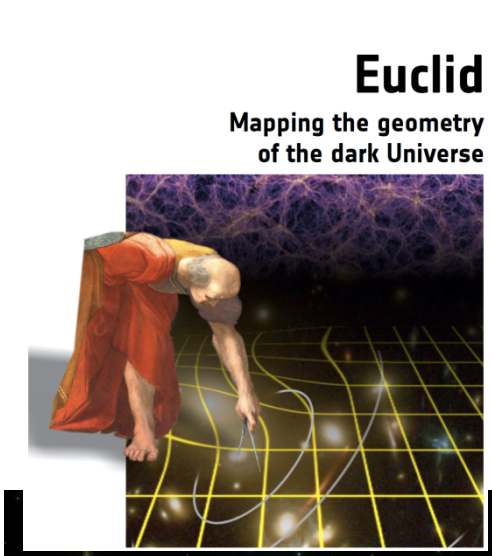

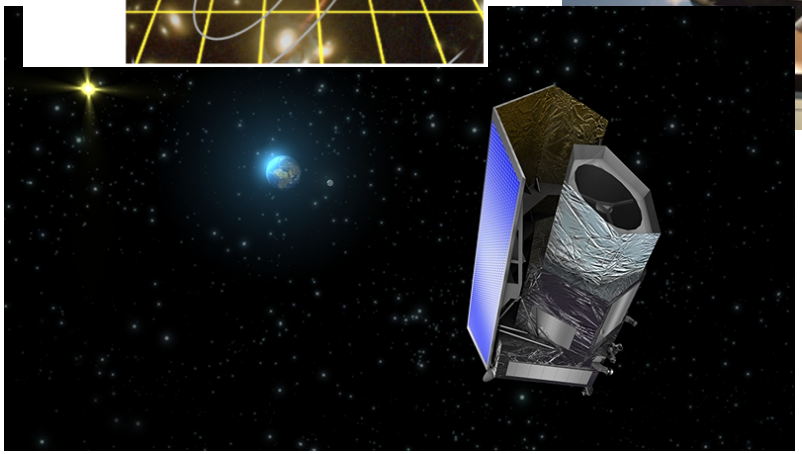

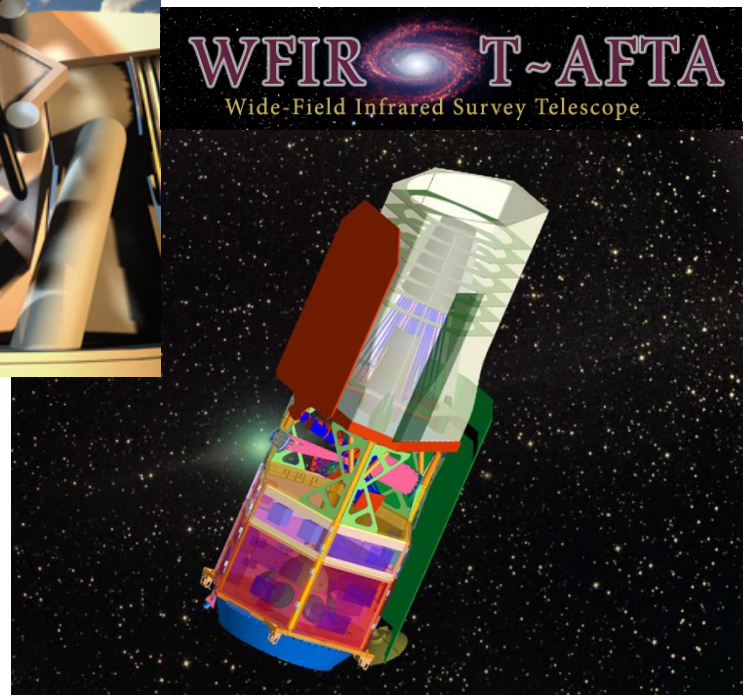

２、SKAによる宇宙論

電波観測による宇宙論

原始密度ゆらぎ

- continuum survey
  → 弱重力レンズ
- HI line survey（近傍宇宙）
  → 銀河分布

} 暗黒エネルギー

- 再イオン化期の中性水素
  - 中性水素密度ゆらぎ
  - 21cm forest

} 早期暗黒エネルギー

z = 0.8のHI intensity mapping

Chang+ 2010

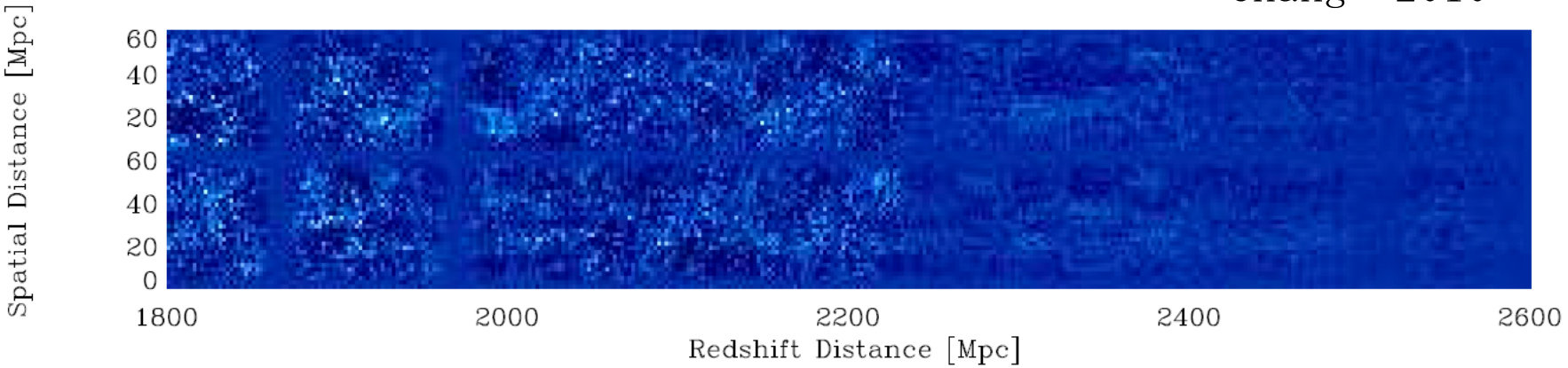

SKA survey

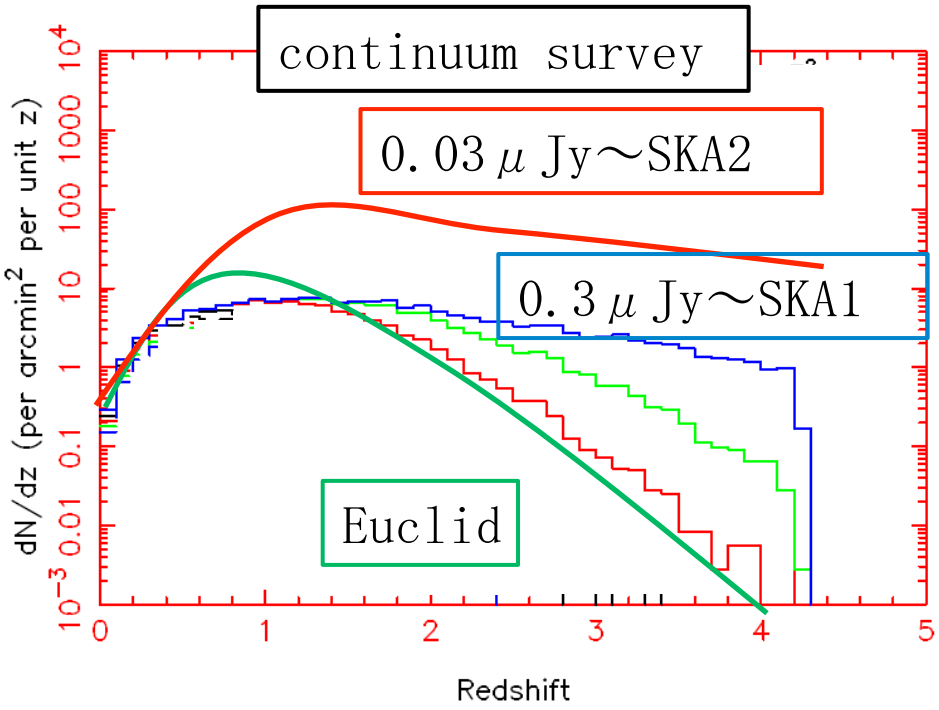

Euclid "Red Book"
Abdalla+ 2010

1yr, 20,000 deg^2
FOV=10 deg^2

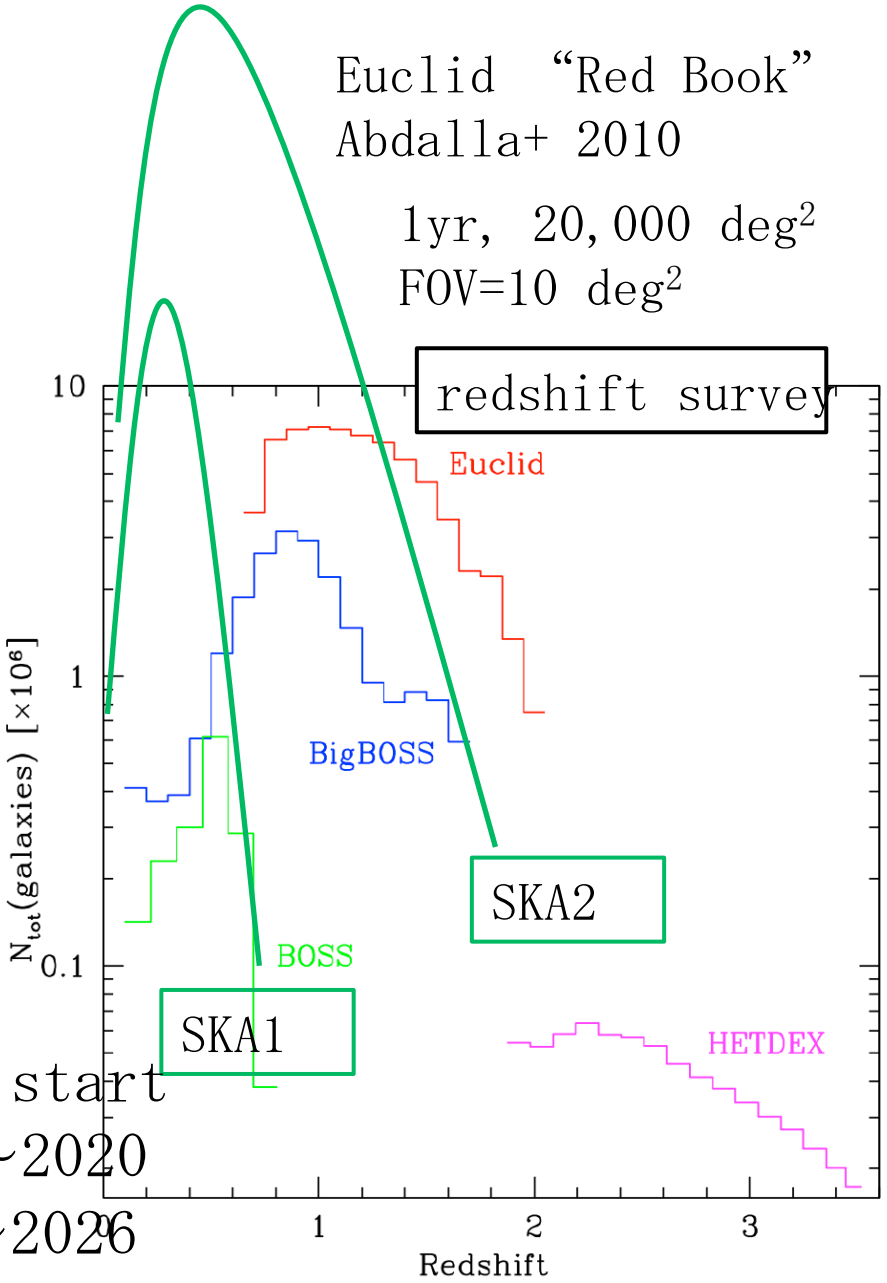

project	redshift	imaging	start
SKA1	10^8	10^9	～2020
SKA2	10^9	10^{10}	～2026
Euclid	10^8	10^9	～2020

非ガウス性

ISW（CMBと銀河の相関）
によるf_{NL}への制限

銀河のパワースペクトル
によるf_{NL}への制限

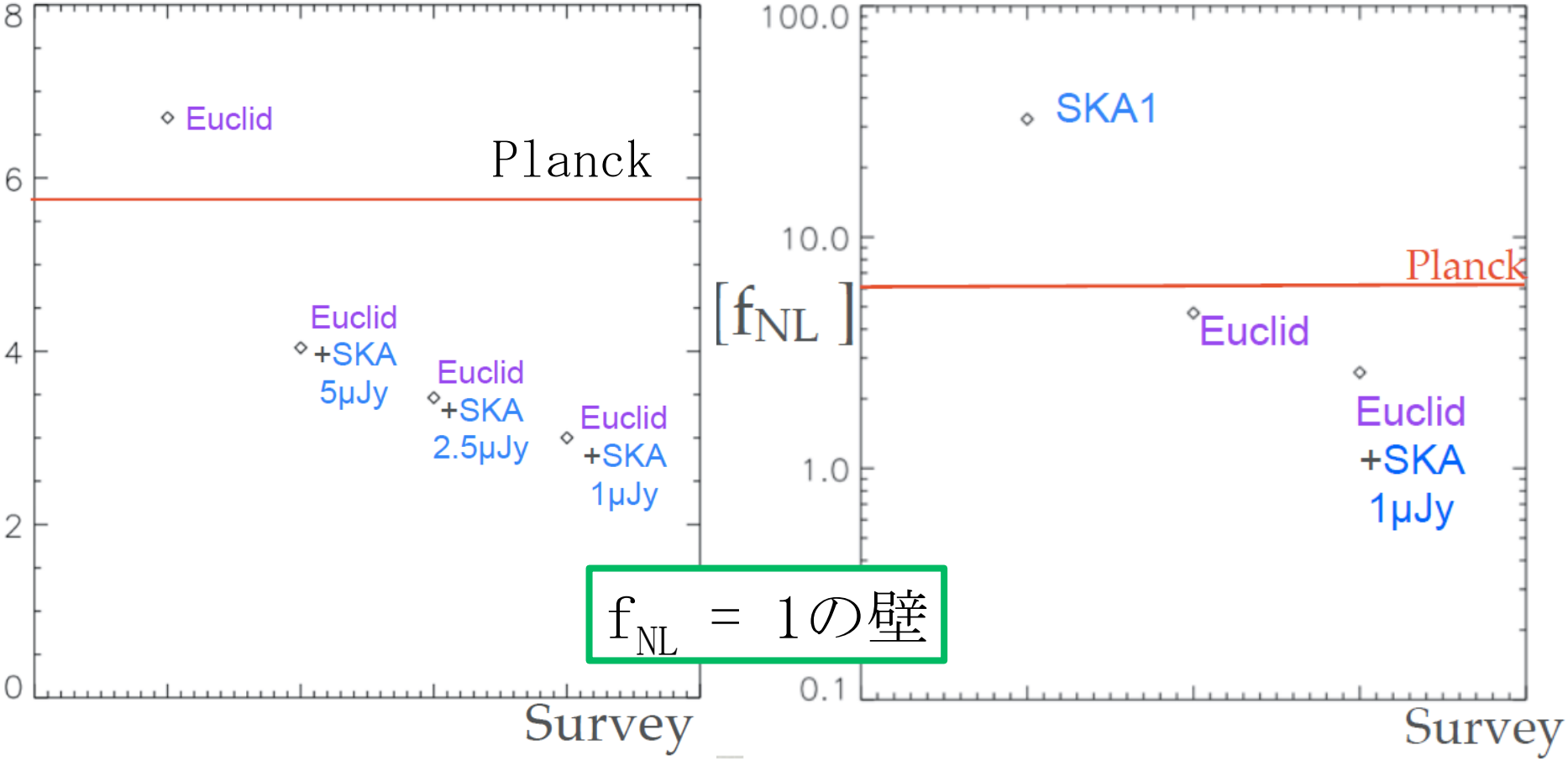

f_{NL} ＝ 1の壁

SKA cosmology team

原始密度ゆらぎの性質

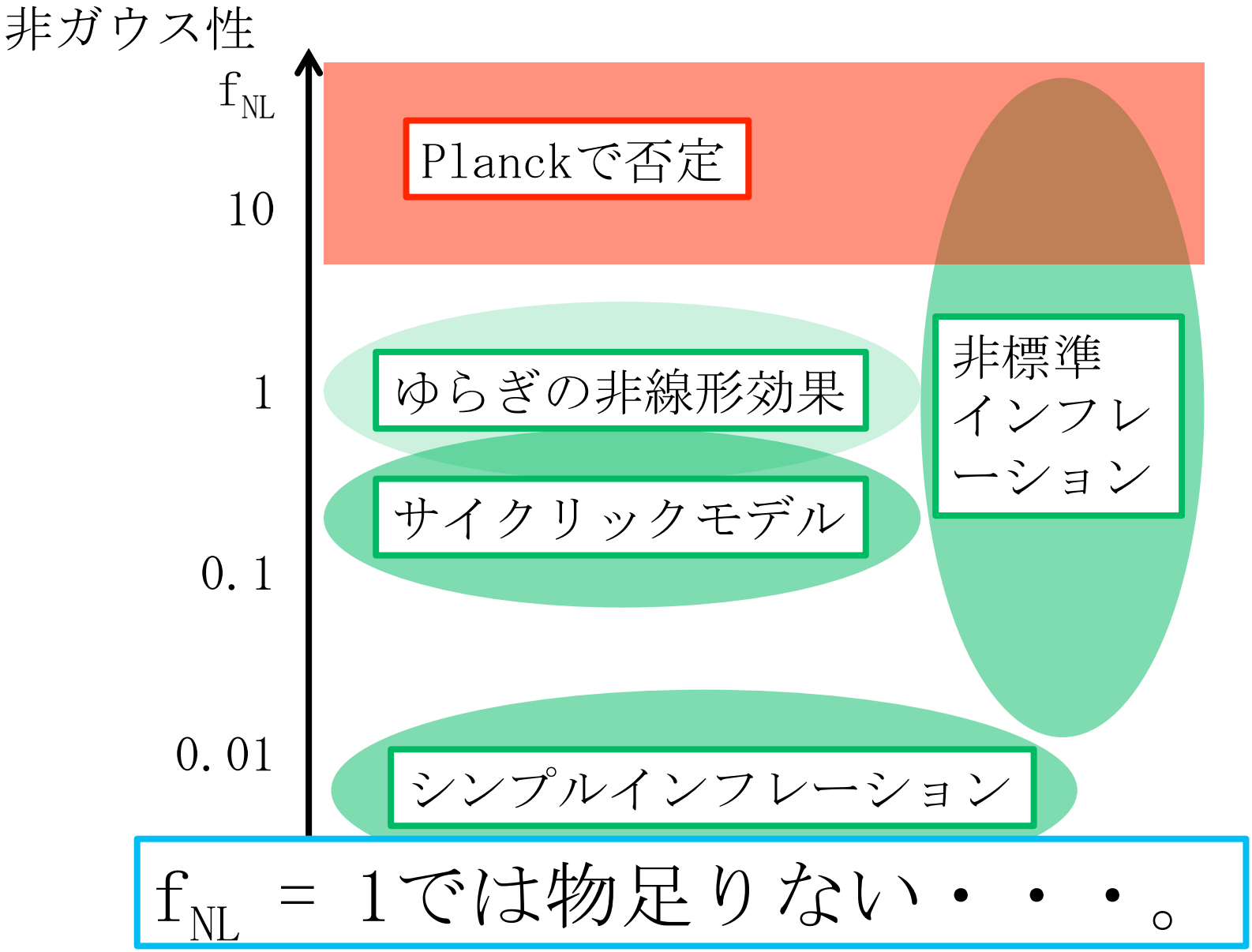
非ガウス性
f_{NL}
10
1
0.1
0.01
Planckで否定
ゆらぎの非線形効果
サイクリックモデル
非標準
インフレ
ーション
シンプルインフレーション
f_{NL} ＝ 1では物足りない・・・。

SKAによる宇宙論

普通にやっていたらはっきり言ってインパクトがない！

- 光赤外にも巨大サーベイがある
- cosmic variance limited

  ↓

  理論の予言は密度ゆらぎの統計的性質
  - 小さなスケールのゆらぎはたくさんのサンプル
  - 宇宙スケールのゆらぎはたった１つのサンプル

cosmic varianceをなんとかしなければ・・・。

3、multi-tracer method

bias

Seljak 2009
cosmic varianceをなくす

DMの分布を知りたいが
観測できるのは天体（バリオン）

bias：天体はDMの濃いところに
できるが、密度ゆらぎは等しくない

$$\delta_g = f(\delta_{\mathrm{DM}}) \approx b\delta_{\mathrm{DM}}$$

大スケールではlinearで
比例定数b = const.

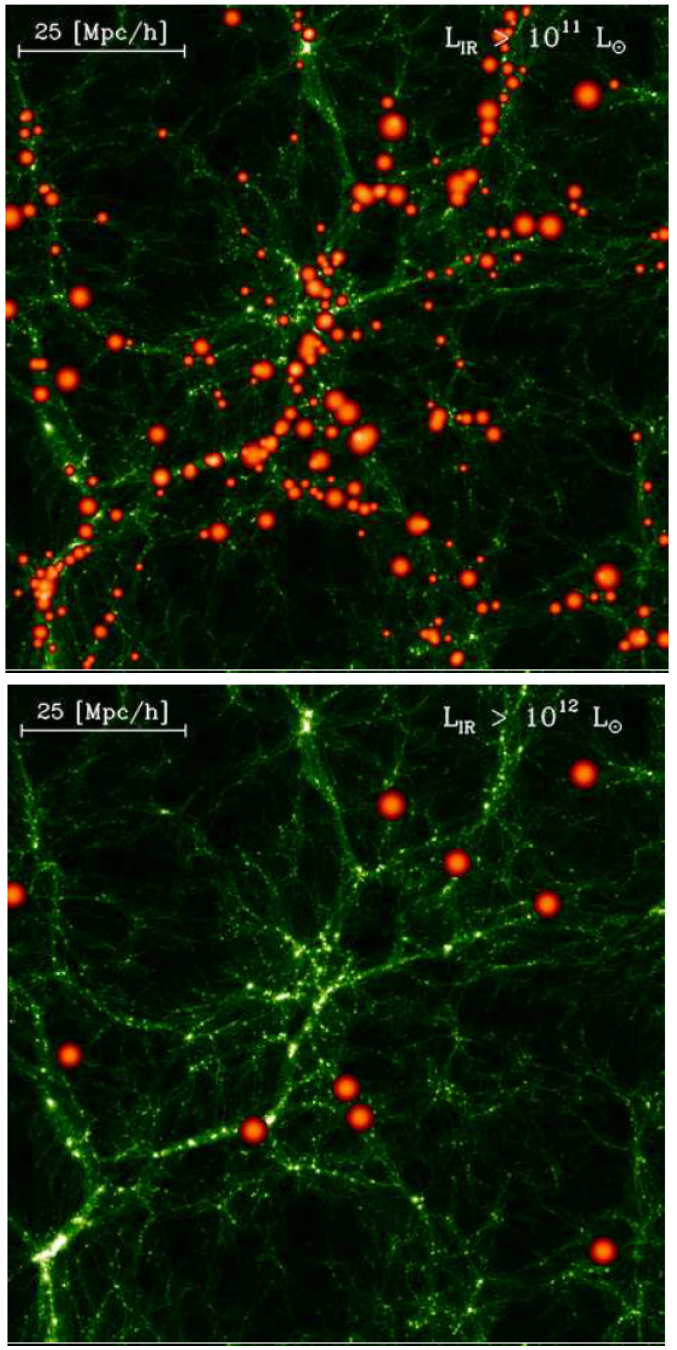

Carlton Baugh

multi-tracerのアイデア

異なるbiasを持つ２つのtracerを考える

$$\delta_1 = b_1 \delta_{\mathrm{DM}}$$
$$\delta_2 = b_2 \delta_{\mathrm{DM}}$$

$$\Rightarrow \quad \frac{b_2}{b_1} = \frac{\delta_2}{\delta_1}$$

ランダム性が消える！
biasはcosmic varianceなしに決まる！

Cole et al. 2005

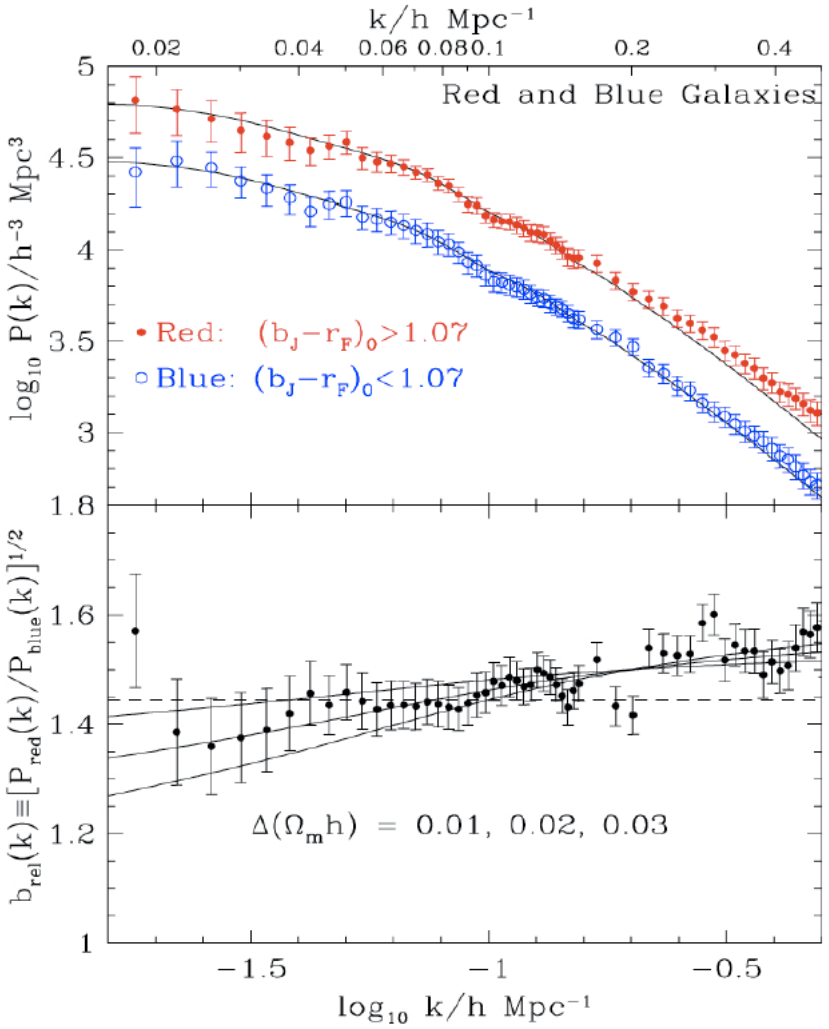

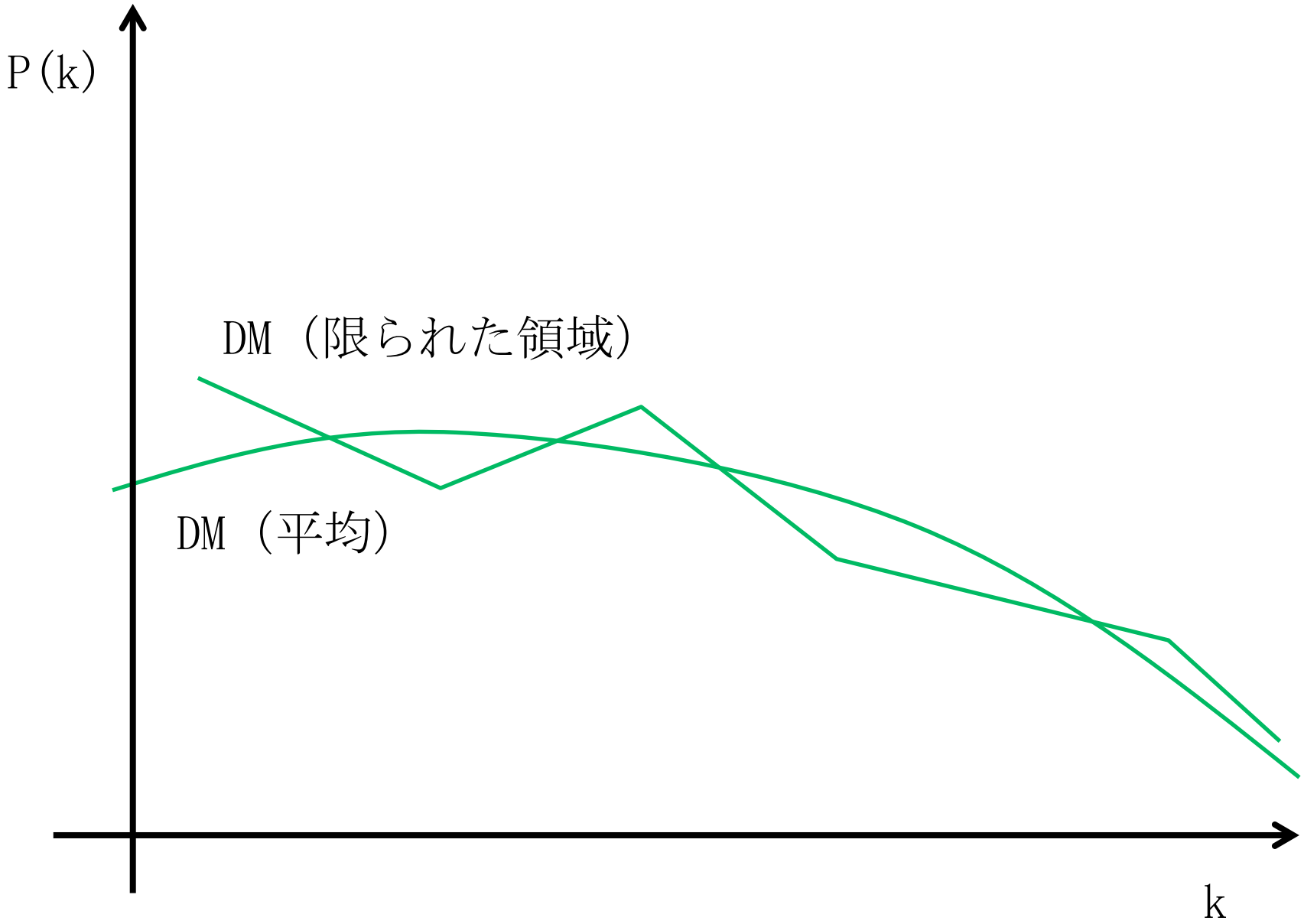
P(k)
DM（限られた領域）
DM（平均）
k

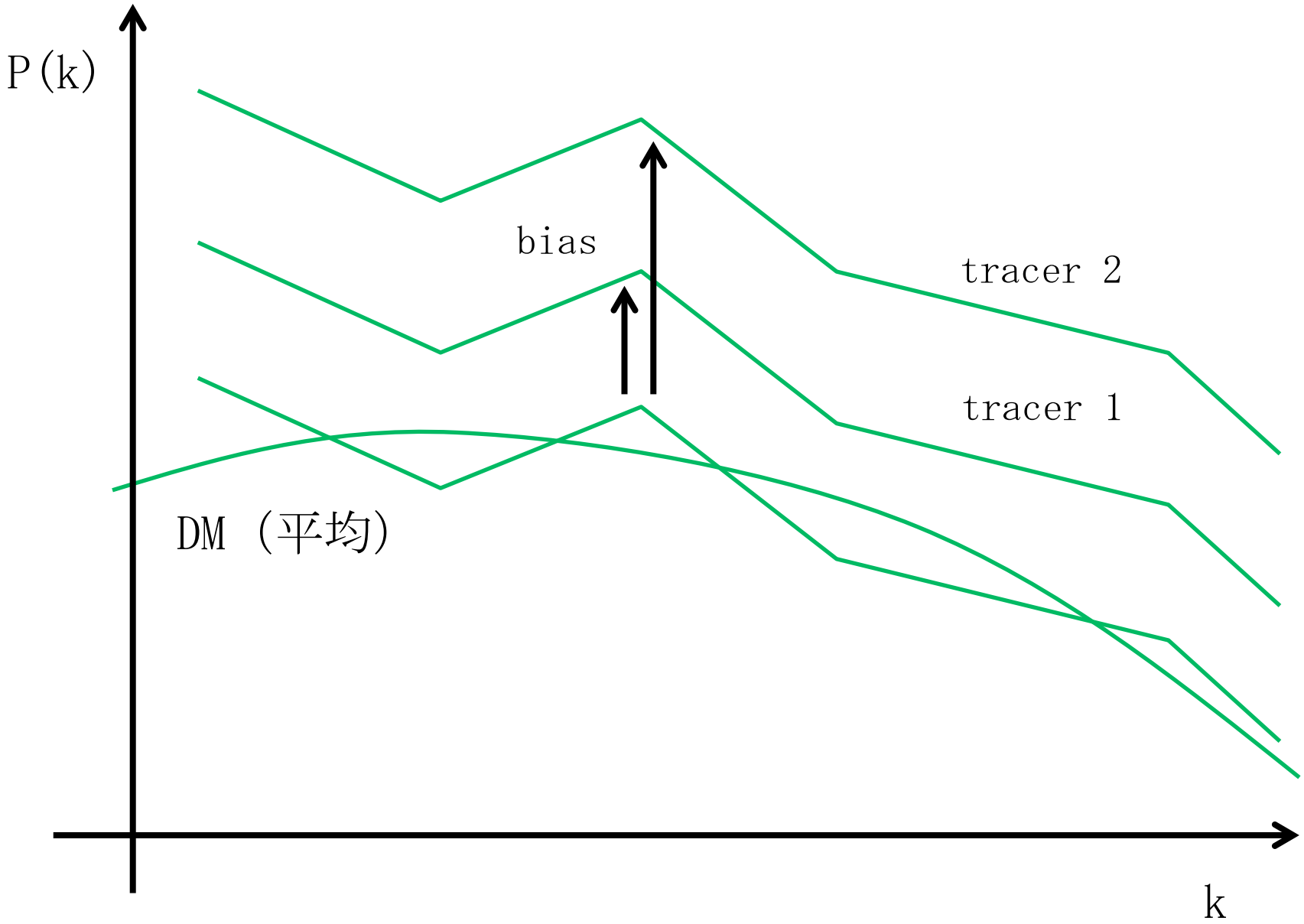
P(k)
bias
tracer 2
tracer 1
DM（平均）
k

DMのP(k)はあまり決まらないが
biasの比はよく決まる。
（ただしbiasがdeterministicのとき）

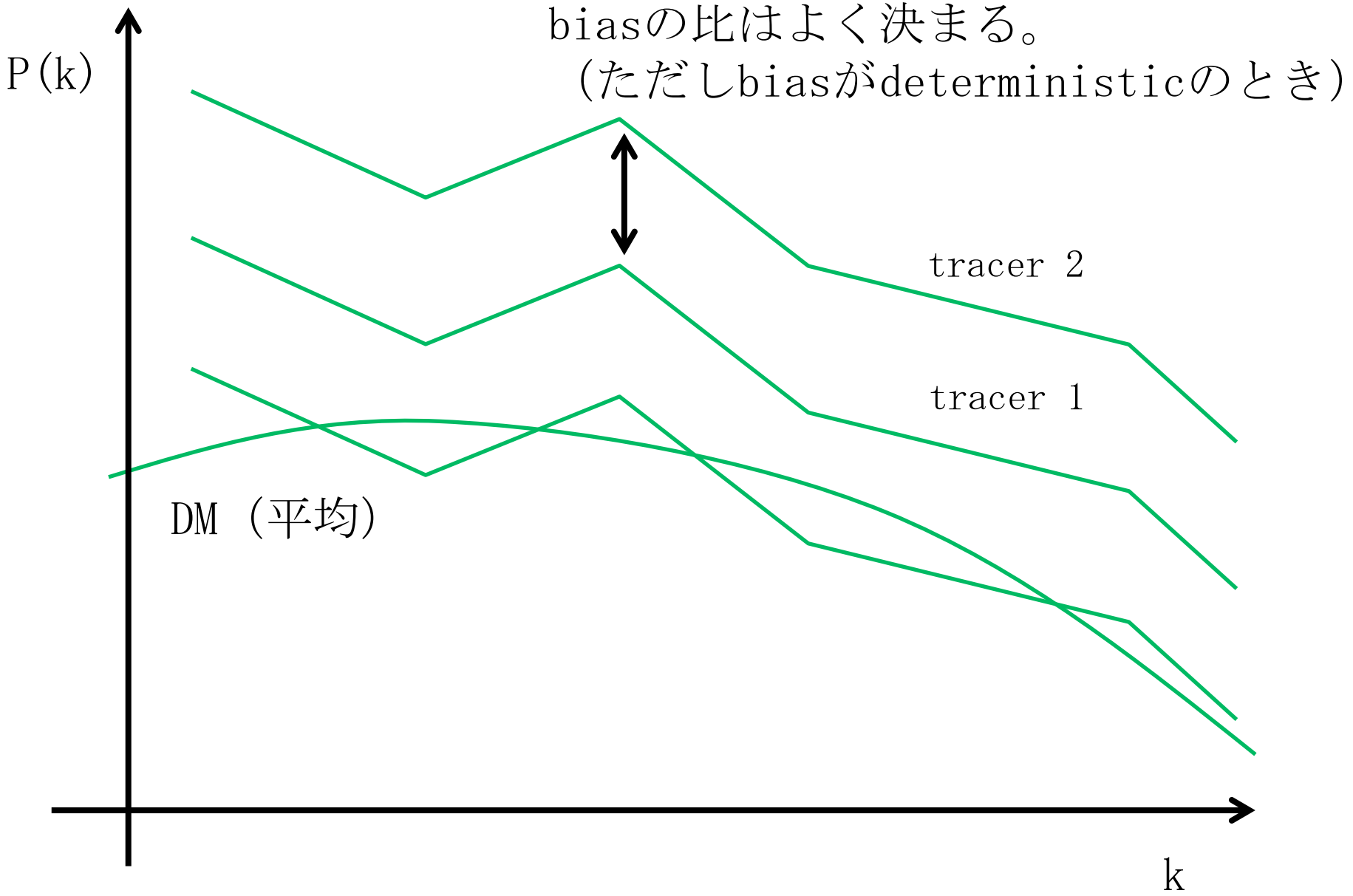

bias with f_{NL}

f_{NL}があるとbiasがスケール依存するようになる

$$P(k) = (b + \Delta b(k) f_{nl})^2 P_{dm}(k),$$

$$\Delta b(k) = 2(b-p)\delta_c \frac{\phi}{\delta} = \frac{3(b-p)\delta_c \Omega_m H_0^2}{c^2 k^2 T(k) D(z)}$$

普通は銀河のP(k)を測ってそこからbiasの情報を引き出すが、P_{DM}自体は重要でない。

２つの異なるbiasを持つ天体があればその比からbiasが精度よく求まる。

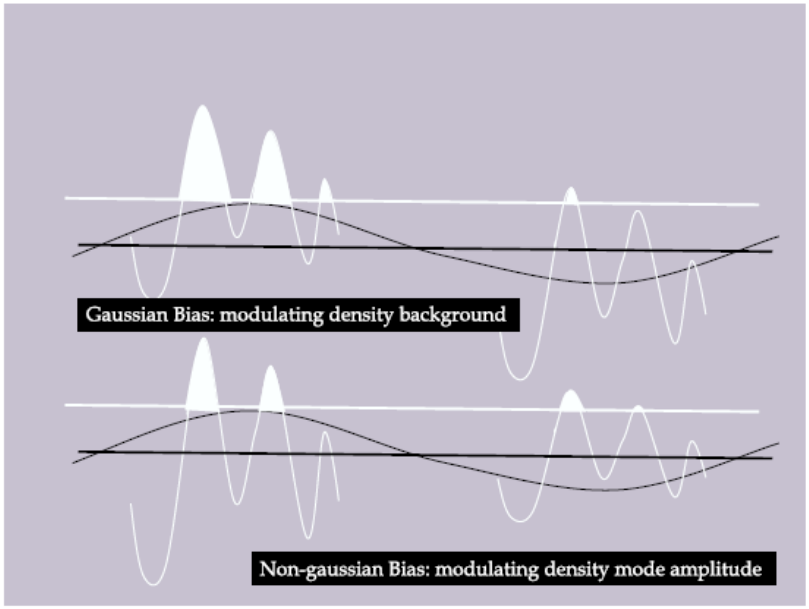

FIG. 5: This figure illustrates the contrast between the gaussian and non-gaussian halo/galaxy bias. The two plots show cartoon versions of linear density vs. spatial position. The white shaded areas indicate collapse regions. For gaussian initial conditions, different Fourier modes are uncorrelated, and so long wavelength modes (thin black curve) only change the background local mean value of small scale modes (thin white curves), which in turn changes the number of density peaks that cross the collapse threshold (thick white line) and form haloes. However, for non-gaussian initial condition, the long wavelength modes can also modulate the amplitude of small scale modes, which causes an additional modulation of collapsed halo density.

Afshordi+ 2008

redshift space distortion

redshift space distortion

redshift surveyでは天体までの距離はわからず
redshiftだけがわかる。
→ 天体の運動の影響が出る

$$\tilde{\delta}_{g,1}(\vec{k}) = (b_1 + f\mu^2)\,\tilde{\delta}_m(\vec{k})$$
$$\tilde{\delta}_{g,2}(\vec{k}) = (b_2 + f\mu^2)\,\tilde{\delta}_m(\vec{k})$$

$$\frac{\tilde{\delta}_{g,1}(\vec{k})}{\tilde{\delta}_{g,2}(\vec{k})} = \frac{1 + \frac{f}{b_1}\mu^2}{\frac{b_2}{b_1} + \frac{f}{b_1}\mu^2}$$

$$f \equiv d\ln D/d\ln a \simeq \Omega_{\rm m}^{\gamma}$$

μ： 視線方向と波数のなす角の余弦

一般相対論だと$\gamma \sim 0.55$、修正重力理論だと異なる値
→ 暗黒エネルギー/修正重力理論を探ることができる

Galaxy And Mass Assembly (GAMA): improved cosmic growth measurements using multiple tracers of large-scale structure

Chris Blake[1⋆], I.K.Baldry[2], J.Bland-Hawthorn[3], L.Christodoulou[4], M.Colless[5], C.Conselice[6], S.P.Driver[7,8], A.M.Hopkins[9], J.Liske[10], J.Loveday[11], P.Norberg[12], J.A.Peacock[13], G.B.Poole[14], A.S.G.Robotham[7,8]

[1] *Centre for Astrophysics & Supercomputing, Swinburne University of Technology, P.O. Box 218, Hawthorn, VIC 3122, Australia*
[2] *Astrophysics Research Institute, Liverpool John Moores University, IC2, Liverpool Science Park, 146 Brownlow Hill, Liverpool, L3 5I*
[3] *Sydney Institute for Astronomy, School of Physics, University of Sydney, NSW 2006, Australia*
[4] *Institute of Cosmology & Gravitation, Dennis Sciama Building, University of Portsmouth, Portsmouth, PO1 3FX, U.K.*
[5] *Research School of Astronomy and Astrophysics, The Australian National University, Canberra, ACT 2611, Australia*
[6] *School of Physics & Astronomy, University of Nottingham, University Park, Nottingham, NG7 2RD, U.K.*
[7] *International Centre for Radio Astronomy Research (ICRAR), University of Western Australia, Crawley, WA 6009, Australia*
[8] *SUPA, School of Physics and Astronomy, University of St Andrews, North Haugh, St Andrews, KY16 9SS, U.K.*
[9] *Australian Astronomical Observatory, P.O. Box 915, North Ryde, NSW 1670, Australia*
[10] *European Southern Observatory, Karl-Schwarzschild-Str. 2, 85748 Garching, Germany*
[11] *Astronomy Centre, University of Sussex, Falmer, Brighton BN1 9QH, U.K.*
[12] *Institute for Computational Cosmology, Department of Physics, Durham University, South Road, Durham DH1 3LE, U.K.*
[13] *Institute for Astronomy, University of Edinburgh, Royal Observatory, Blackford Hill, Edinburgh EH9 3HJ, U.K.*
[14] *School of Physics, University of Melbourne, Parkville, VIC 3010, Australia*

24 September 2013

ABSTRACT

We present the first application of a 'multiple-tracer' redshift-space distortion (RSD) analysis to an observational galaxy sample, using data from the Galaxy and Mass Assembly survey (GAMA). Our dataset is an $r < 19.8$ magnitude-limited sample of 178,579 galaxies covering redshift interval $z < 0.5$ and area 180 deg^2. We obtain improvements of 10-20% in measurements of the gravitational growth rate compared to a single-tracer analysis, deriving from the correlated sample variance imprinted in the distributions of the overlapping galaxy populations. We present new expressions for the covariances between the auto-power and cross-power spectra of galaxy samples that are valid for a general survey selection function and weighting scheme. We find no evidence for a systematic dependence of the measured growth rate on the galaxy tracer used, justifying the RSD modelling assumptions, and validate our results using mock catalogues from N-body simulations. For multiple tracers selected by galaxy colour, we measure normalized growth rates in two independent redshift bins $f\sigma_8(z = 0.18) = 0.36 \pm 0.09$ and $f\sigma_8(z = 0.38) = 0.44 \pm 0.06$, in agreement with standard GR gravity and other galaxy surveys at similar redshifts.

Key words: surveys, large-scale structure of Universe, cosmological parameters

GAMA survey

GAMA (Galaxy and Mass assembly) survey

- Anglo-Australian Telescope
- r < 19.8
- ３つの12×5 deg^2 field
- 185052 targets
- z < 0.25, z > 0.25に分けて解析
- それぞれでcolor, luminosityで２分割してmulti-tracerとして使う

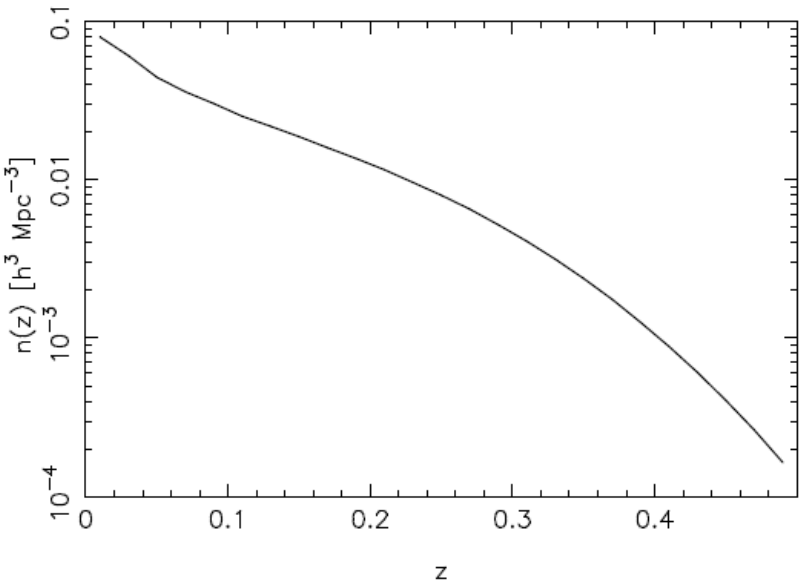

Figure 1. The average number density of GAMA galaxies as a function of redshift. This plot is constructed by combining data in the three survey regions.

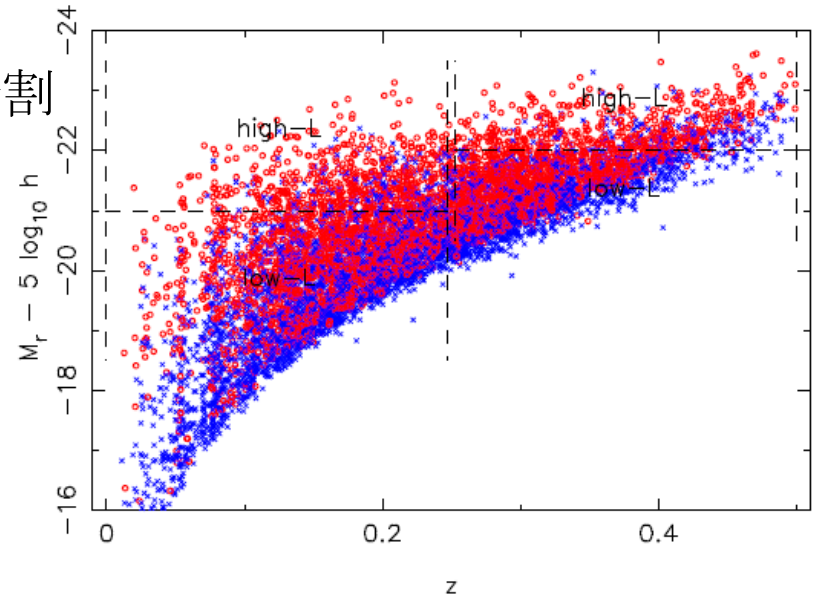

Figure 2. The distribution of absolute magnitudes M_r and redshifts z for the GAMA galaxies used in our analysis, which satisfy the selection criteria described in the text. The blue and red colour subsamples are plotted as crosses and open circles, respectively, and illustrated by appropriate colouring of the data points. The 'high-L' and 'low-L' subsamples are shown by the ranges indicated on the figure. In this plot, the galaxies have been randomly subsampled by a factor of 20, for clarity.

２つのtracerの実空間分布

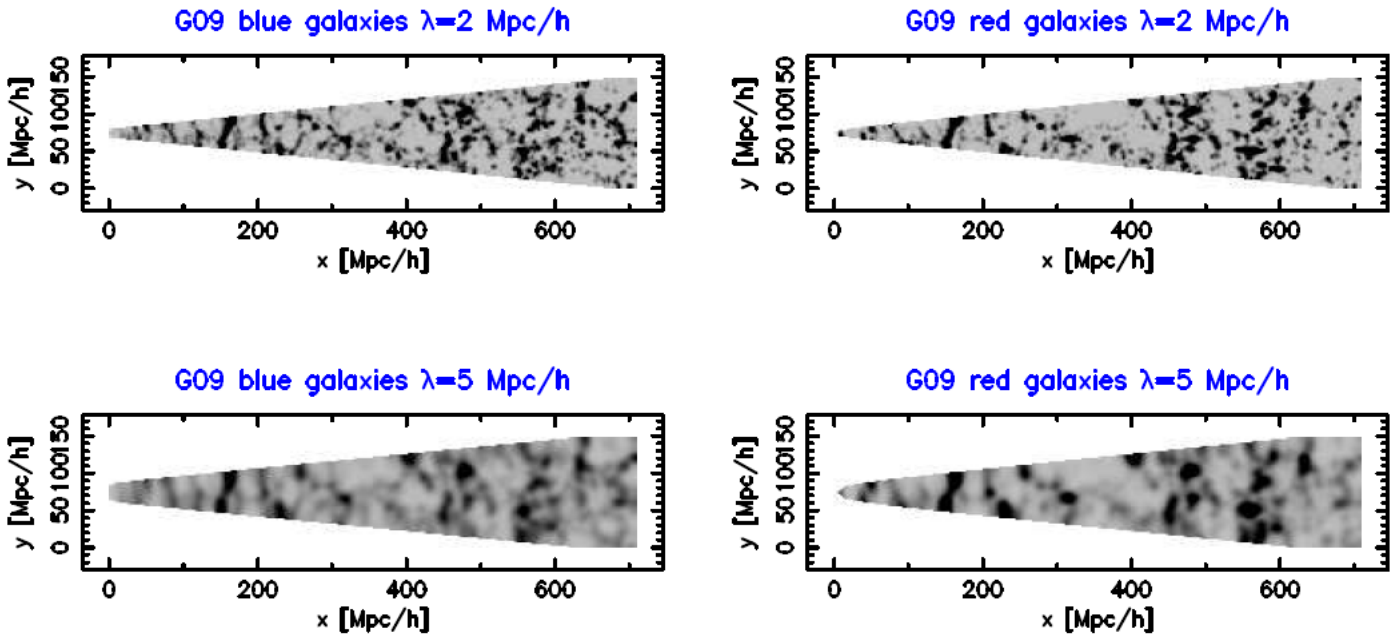

Figure 5. The galaxy overdensity field within the G09 region, determined from the gridded data and selection function, and projected onto a 2D plane parallel to the line-of-sight (such that the x-, y- and z-axes are oriented in the redshift, right ascension and declination directions, respectively). The left-hand and right-hand panels show the measurements for blue and red galaxies, respectively. The top and bottom rows illustrate two choices of smoothing scale, 2 and $5\,h^{-1}$ Mpc. Qualitatively, it can be seen that the different galaxy subsamples are tracing the same underlying large-scale structure.

2つのtracerのフーリエモードの相関

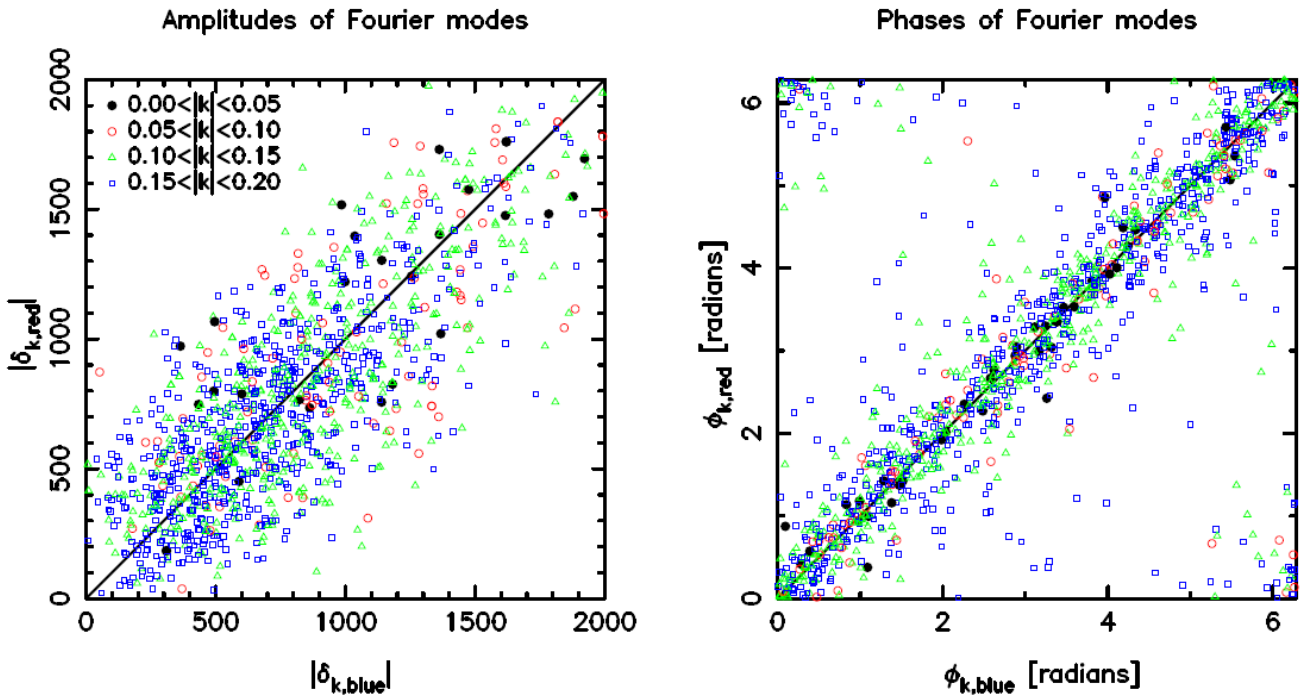

Figure 7. A mode-by-mode comparison of the moduli $|\tilde{\delta}(\vec{k})|$ and phases $\phi(\vec{k})$ of the complex Fourier amplitudes $\tilde{\delta}(\vec{k})$ estimated for the red and blue galaxy subsamples for the redshift interval $0 < z < 0.25$. The points are coded by plotting symbol and colour into four wavenumber bins in the range $k < 0.2\,h$ Mpc^{-1}. We note the strong correlations between the measurements of a given Fourier amplitude for the two different tracers. In the right-hand panel, the data points which appear in the upper-left and lower-right corners result from the 2π wrapping of the phases and support the correlation.

モデルフィット

$$P_\alpha(k,\mu) = P_{\delta\delta}(k)\ \left(b_\alpha + f\mu^2\right)^2\ e^{-k^2\mu^2\sigma_v^2/H_0^2}$$

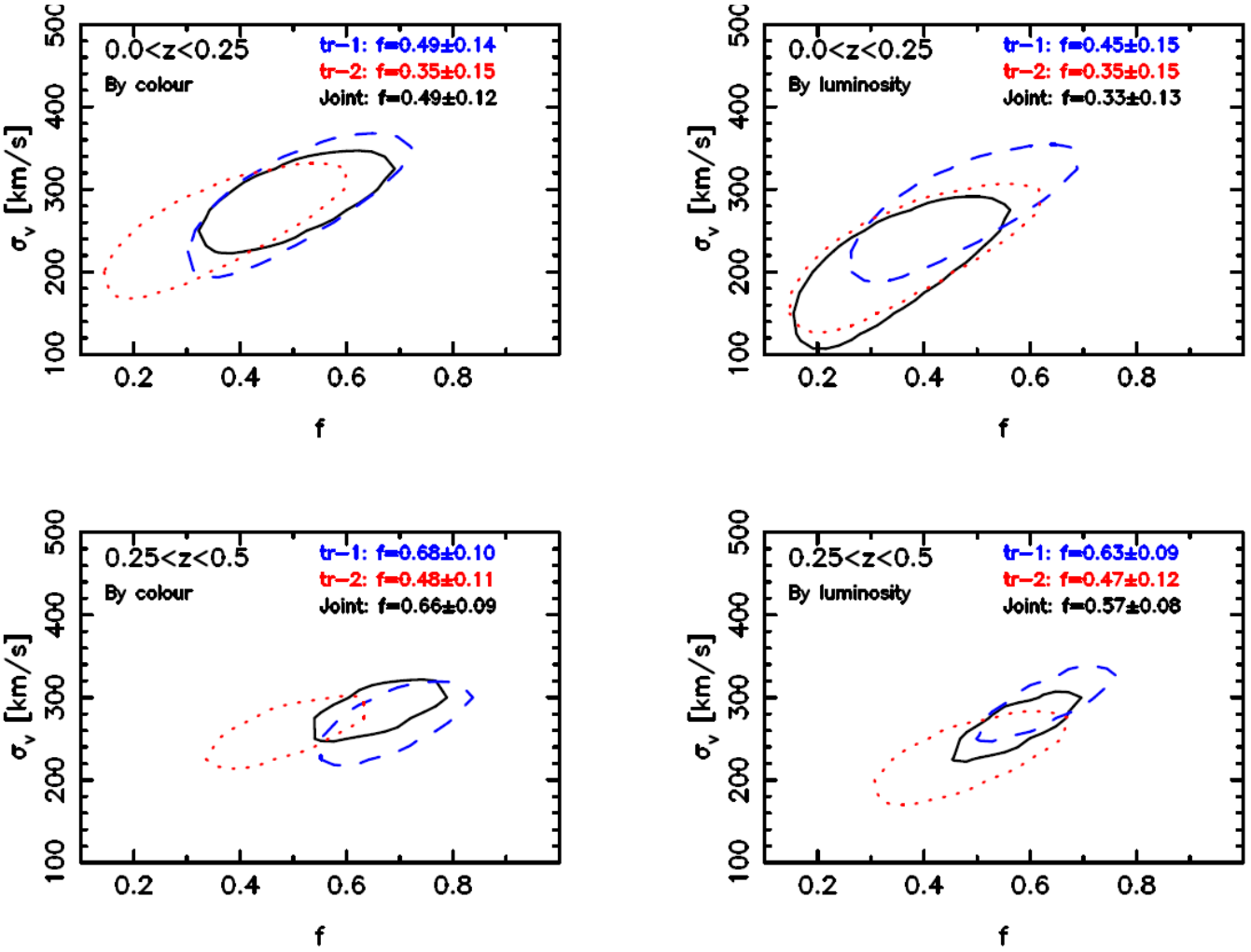

Figure 11. Fits for the RSD parameters (f, σ_v), marginalized over galaxy bias, for different redshift ranges and multiple-tracer subsamples (split by both colour and luminosity). In each case we compare the fits to the individual subsamples (blue dashed and red dotted contours for the low-bias ('tr-1') and high-bias ('tr-2') sample, respectively) and the joint sample (black solid contours). The likelihood contours are all 68% confidence regions. The captions quote the 1D marginalized measurements of the growth rate.

growth rate

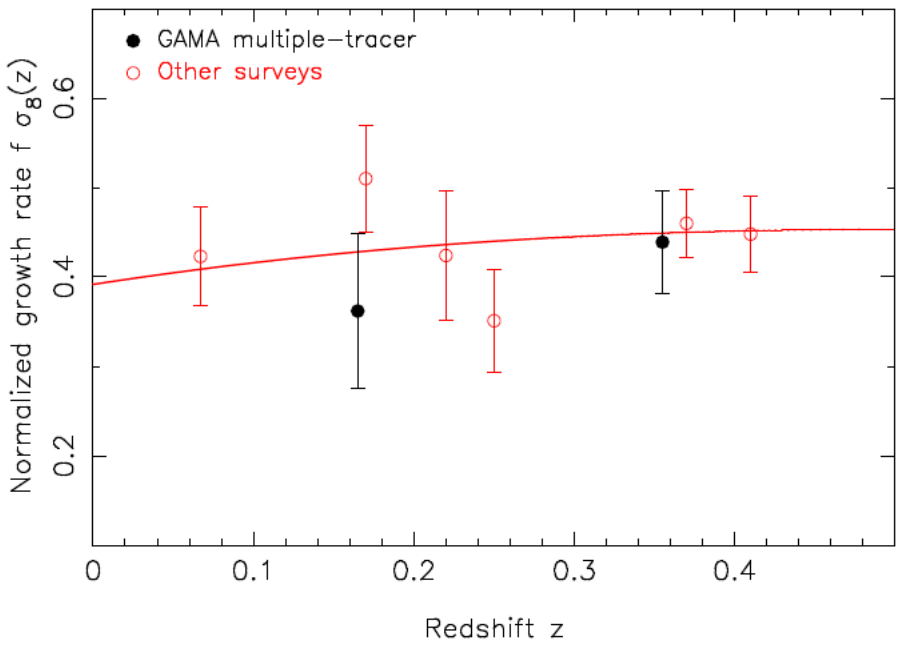

Figure 12. Marginalized measurements of the normalized growth rate $f\sigma_8(z)$ fit to multiple-tracer GAMA galaxy subsamples split by colour. The prediction of a flat ΛCDM model with matter density $\Omega_m = 0.27$ and normalization $\sigma_8 = 0.8$ is also shown as the solid line. The open squares display the results of RSD analyses of a series of other galaxy surveys in a similar redshift range, taken from 6dFGS ($z = 0.067$, Beutler et al. 2012), 2dFGRS ($z = 0.17$, Hawkins et al. 2003), the SDSS Luminous Red Galaxy sample ($z = 0.25$ and $z = 0.37$, Samushia et al. 2012) and the WiggleZ Survey ($z = 0.22$ and $z = 0.41$, Blake et al. 2011).

このデータではあまり
multi-tracerのよさが
発揮されていない。

Radio Galaxy populations and the multi-tracer technique: pushing the limits on primordial non-Gaussianity

L. D. Ferramacho[1,2⋆], M. G. Santos[2,1,3], M. J. Jarvis[4,2] and S. Camera[1,2]
[1] *CENTRA, Instituto Superior Técnico, Universidade de Lisboa, Av. Rovisco Pais 1, 1049-001, Lisboa, Portugal.*
[2] *Department of Physics, University of Western Cape, Cape Town 7535, South Africa.*
[3] *SKA SA, 3rd Floor, The Park, Park Road, Pinelands, 7405, South Africa*
[4] *Astrophysics, Department of Physics, Keble Road, Oxford OX1 3RH, UK.*

February 12, 2014

ABSTRACT

We explore the use of different radio galaxy populations as tracers of different mass halos and therefore, with different bias properties, to constrain primordial non-Gaussianity of the local type. We perform a Fisher matrix analysis based on the predicted auto and cross angular power spectra of these populations, using simulated redshift distributions as a function of detection flux and the evolution of the bias for the different galaxy types (Star forming galaxies, Starburst galaxies, Radio-Quiet Quasars, FRI and FRII AGN galaxies). We show that such a multi-tracer analysis greatly improves the information on non-Gaussianity by drastically reducing the cosmic variance contribution to the overall error budget. By using this method applied to future surveys, we predict a constraint of $\sigma_{f_{nl}} = 3.6$ on the local non-Gaussian parameter for a galaxy detection flux limit of 10μJy and $\sigma_{f_{nl}} = 2.2$ for 1 μJy. We show that this significantly improves on the constraints obtained when using the whole undifferentiated populations ($\sigma_{f_{nl}} = 48$ for 10 μJy and $\sigma_{f_{nl}} = 12$ for 1 μJy). We conclude that continuum radio surveys alone have the potential to constrain primordial non-Gaussianity to an accuracy at least a factor of two better than the present constraints obtained with Planck data on the CMB bispectrum, opening a window to obtain $\sigma_{f_{nl}} \sim 1$ with the Square Kilometer Array.

Key words: large-scale structure of Universe – cosmological parameters – inflation – cosmology: observations – radio continuum: galaxies

SKAでいろんな電波天体を観測してmulti-tracerを適用する

$$b_h(M,z) = b_L(M,z) + f_{nl}\delta_c\left[(b_L(M,z)-1\right]\frac{3\Omega_m H_0^2}{c^2k^2T(k)D(z)}$$

- Star forming galaxies (SFR): $M_{halo}=1\times10^{11}h^{-1}M_\odot$
- Starbursts (SB): $M_{halo}=5\times10^{13}h^{-1}M_\odot$
- Radio Quiet Quasars (RQQ): $M_{halo}=3\times10^{12}h^{-1}M_\odot$ → ほんと？
- Radio loud AGN (FRI): $M_{halo}=1\times10^{13}h^{-1}M_\odot$
- Radio loud AGN (FRII): $M_{halo}=1\times10^{14}h^{-1}M_\odot$

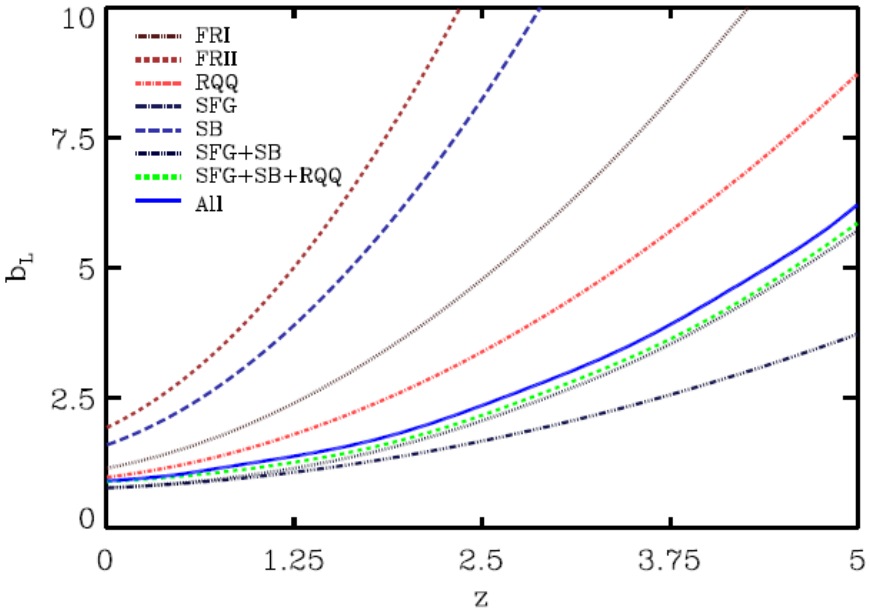

Figure 2. Bias redshift evolution for the different source combinations considered in this paper, considering a Gaussian distribution of galaxies around the central masses as discussed section 3.2. When combining populations, the bias is obtained through eq. 12.

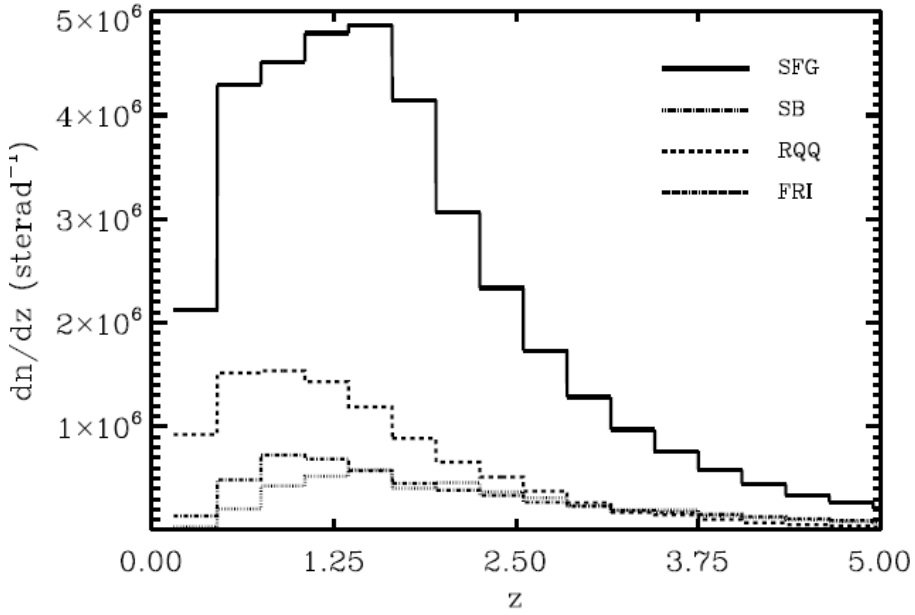

Figure 3. Redshift distribution of sources per steradian for SKA phase-1 (Flux cut detection at 5 μJy). The source types are Star Forming Galaxies (SFG), Starburst galaxies (SB), Radio quiet quasars (RQQ) and FRI. We omit the distribution for FRII galaxies since their number is much lower (of the order of 100) and would not be visible in this figure. All distributions were obtained form the S^3 catalogs down to a sensitivity limit of 1μJy and applying a cut at 5σ.

- Star forming galaxies (SFR): $M_{halo}=1\times10^{11}h^{-1}M_{\odot}$
- Starbursts (SB): $M_{halo}=5\times10^{13}h^{-1}M_{\odot}$
- Radio Quiet Quasars (RQQ): $M_{halo}=3\times10^{12}h^{-1}M_{\odot}$
- Radio loud AGN (FRI): $M_{halo}=1\times10^{13}h^{-1}M_{\odot}$
- Radio loud AGN (FRII): $M_{halo}=1\times10^{14}h^{-1}M_{\odot}$

観測的にどう区別するか？

・FRI/FRII：ジェットの形の違い。1 arcsecでの分解が必要。

・SFR/SB：星形成率の違いだけ。電波だけでは判断しがたい。

・RQQ/SFR/SB：RQQはX線も出すのでX線で区別。

→ RQQ/SFR/SBは区別できる場合とできない場合を考える

Fisher解析でf_{NL}の制限を予言

- SKA phase 1
- redshiftの情報なし
- 天体の種類が区別できない場合も想定する

$$\{\Omega_m; h; \log 10^{10A_s}; f_{nl}; M_{cent}^{SFG}; M_{cent}^{SB}; M_{cent}^{RQQ}; M_{cent}^{FRI}; M_{cent}^{FRII}\}$$

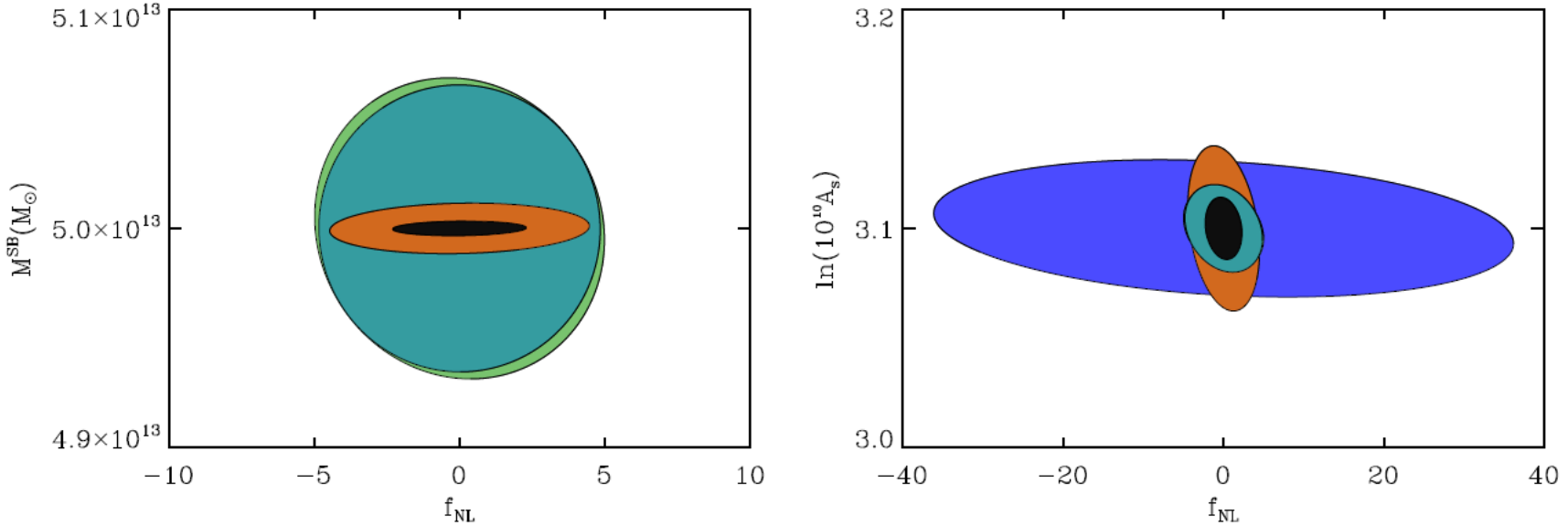

Figure 4. 1-σ forecasts on f_{nl} and central mass for starburst population (*left*) and on f_{nl} and primordial fluctuation amplitude (*right*), both for a flux cut detection at 5 μJy. Larger blue ellipse considers the whole sample of galaxies and light green ellipses represent the constrains if we consider the combination of SFG, SB and RQQ (or just SFG and SB, in light blue) as one single undifferentiated population with bias defined by eq. 12. The orange contour corresponds to the constraint using the whole differentiated 5 galaxy population for z<1 and 4 bins with SFG and SB undifferentiated for z>1. Finally, the smaller and darker ellipse shows the ideal case where all 5 populations could be differentiated over the entire redshift range.

	$\sigma_{f_{nl}}$				
Flux detection threshold	Full sample[a]	3 bins	4	4+5 bins	5 bins
1 μJy	12 (9.6)	2.8	2.7	2.2	0.7
3 μJy	25 (17)	2.7	2.7	2.6	1.2
5 μJy	32 (23)	3.3	3.2	2.9	1.5
10 μJy	48 (35)	3.7	3.7	3.6	1.9

Table 1. Forecasts on f_{nl} 1-σ errors using the angular power spectra of different galaxy populations for different detection flux limits. We present the results obtained using the full sample of objects with an averaged effective bias and those obtained using the combination of 3 populations of radio galaxies (where SRG, SB and RQQ correspond to one population group), using 4 populations (where only SFG and SB are undifferentiated) and with a selection of 5 populations for z<1 and 4 populations for z> 1 (again with undifferentiated SFG and SB). We also show the result for the ideal case where all 5 populations could be differentiated over the entire redshift range of the survey.
[a] Values in parentheses were obtained assuming a constant and single mass for each sub-population.

観測的にどう区別できるか？
3：（SFR, SB, RQQ）
4：（SFR, SB）, RQQ
5：SFR, SB, RQQ
4+5：5（z<1）, 4（z>1）

biasの違いが大きく
たくさんある天体の区別が重要
→ high zでのSFRとSB

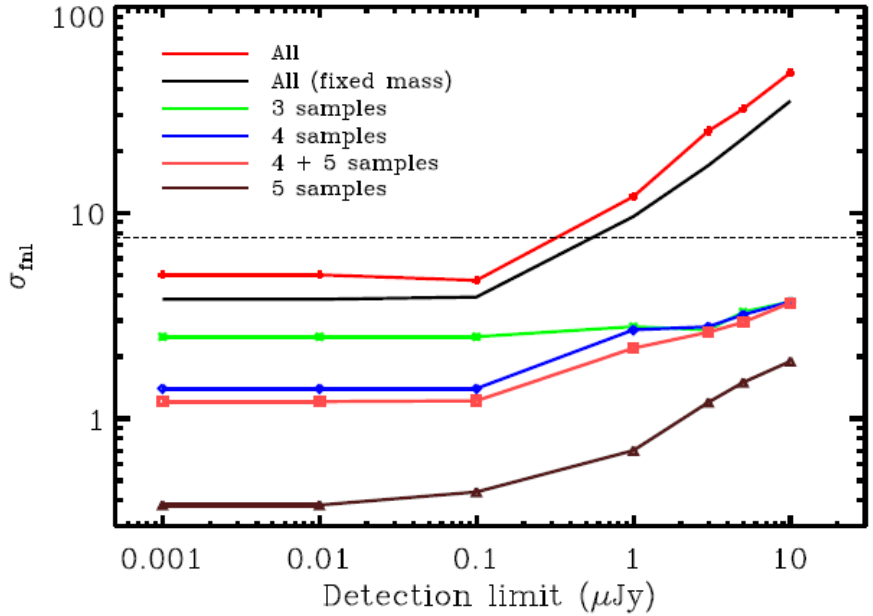

Figure 5. Forecasted constraints on f_{nl} obtained with the multi-tracer method as a function of the flux cut used to detect galaxies. The horizontal line represents the best constrain obtained by the Planck collaboration (Planck collaboration 2013b) normalized to the convention we are using here.

４、まとめ

まとめとできそうなこと

まとめ

- f_{NL}はインフレーション最後の予言
- biasのスケール依存性、質量依存性からf_{NL}に制限
- biasの差が大きく、数が多いほど有利
- SKAだけで$f_{NL} \sim 0.1$

できそうなこと

- redshiftの情報が得られたら？
- 他の分類方法
- higher-order statistics
- 光赤外のサーベイと組み合わせると？
  - 他の種類の天体
  - 弱重力レンズなどで質量の見積もり

→ $f_{NL} \sim 0.01$までいける？

非ガウス性への制限

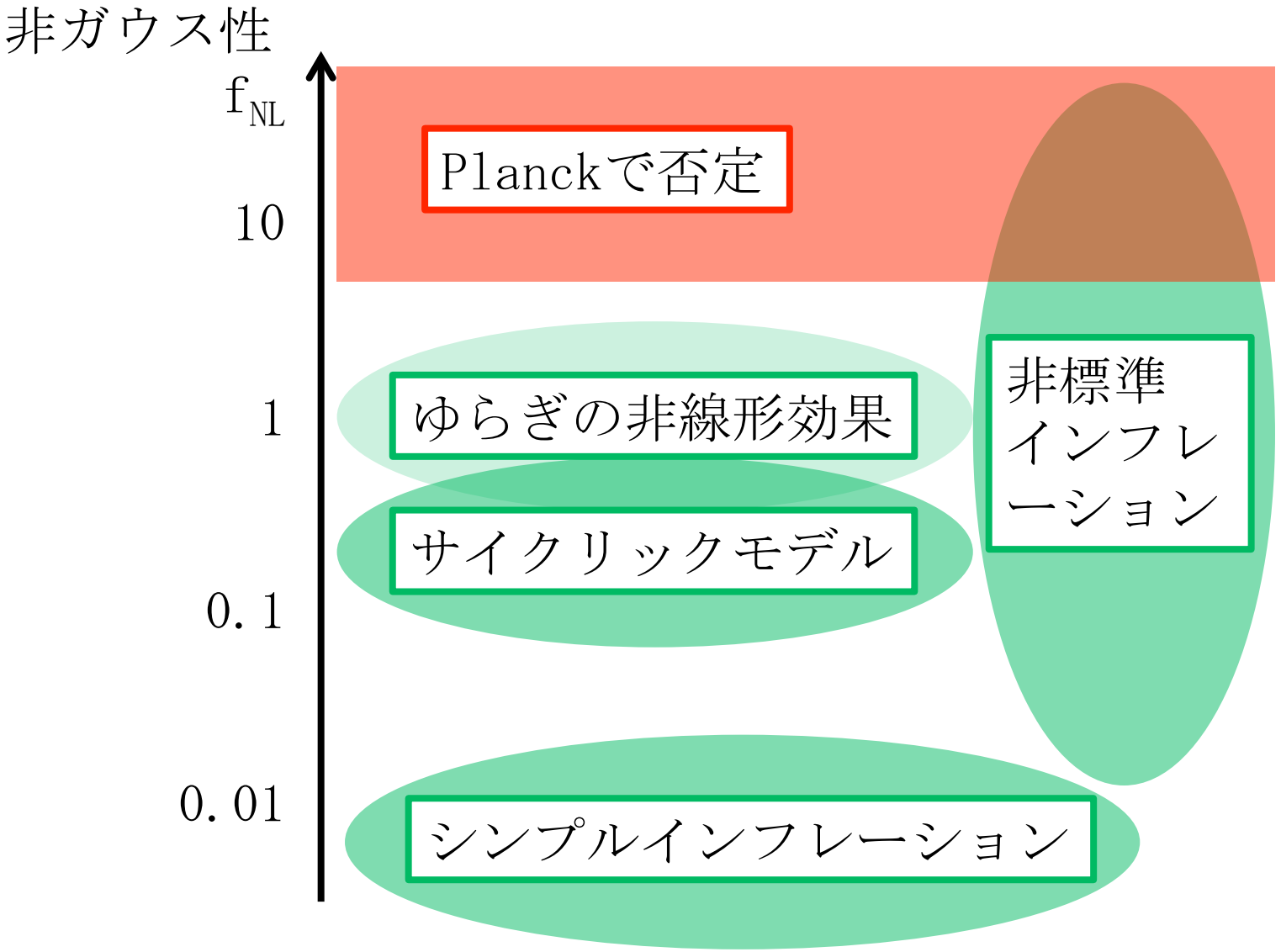
非ガウス性
f_{NL}
10
1
0.1
0.01
Planckで否定
ゆらぎの非線形効果
サイクリックモデル
非標準
インフレ
ーション
シンプルインフレーション

非ガウス性への制限

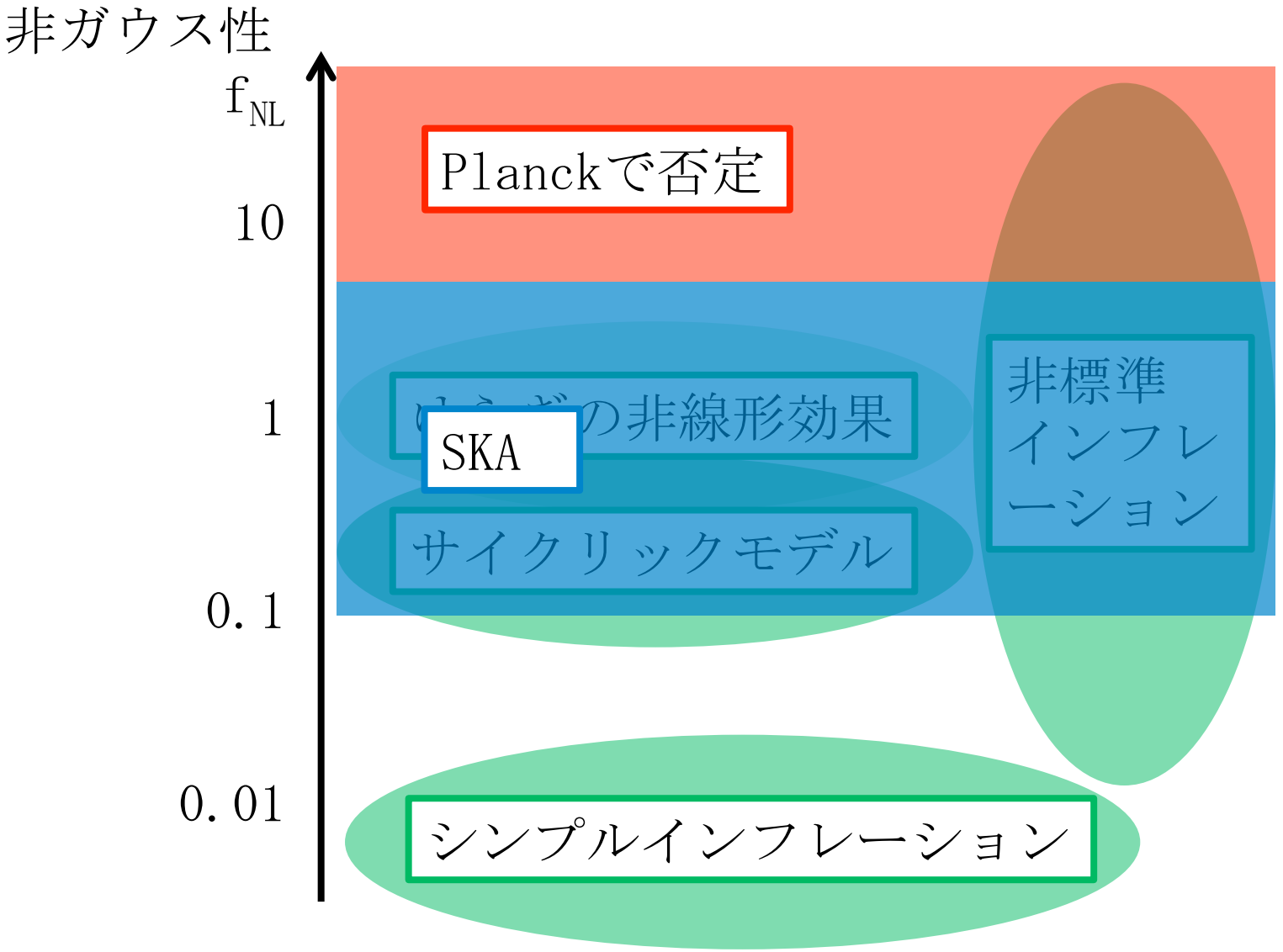
非ガウス性
f_{NL}
10
1
0.1
0.01
Planckで否定
の非線形効果
SKA
サイクリックモデル
非標準
インフレ
ーション
シンプルインフレーション

非ガウス性への制限

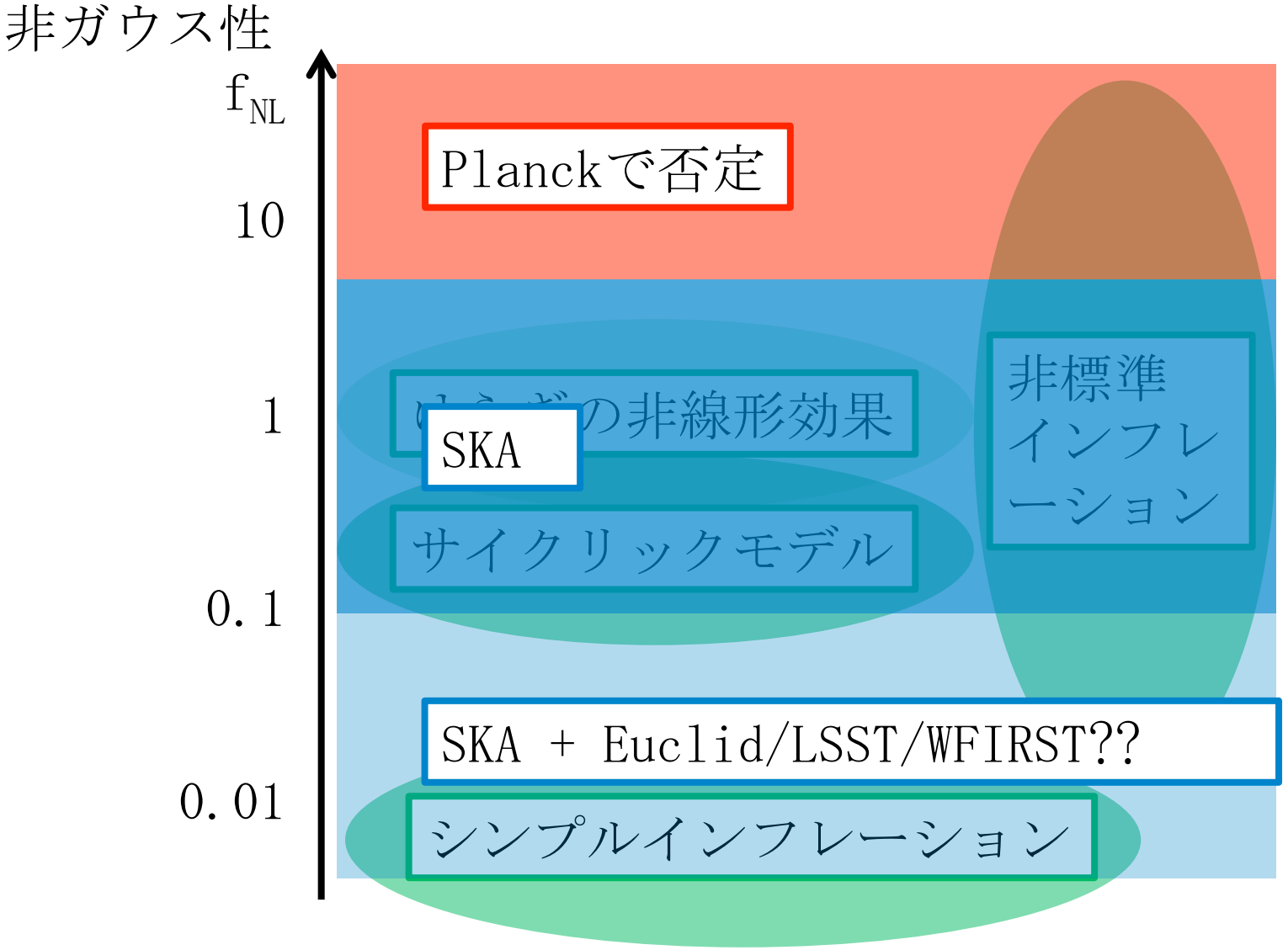
非ガウス性
f_{NL}
10
1
0.1
0.01
Planckで否定
の非線形効果
SKA
サイクリックモデル
非標準
インフレ
ーション
SKA + Euclid/LSST/WFIRST??
シンプルインフレーション